Abstract

A series of eight mononuclear copper(II) complexes [Cu(bdmpe/bpmpe)X]Y [X = Cl / Br and Y = PF_6^-/ BF_4^-] and two binuclear nickle(II) complexes [Ni(bdmpe)μ-Cl]$_2$(Y)$_2$.CH_3CN have been synthesized by the reaction of metal halides precursors with ligands *N*,*N*-bis((3,5-dimethyl-*1H*-pyrazol-1-yl)methyl)-2-(phenylthio)ethan-1-amine (bdmpe) or *N*,*N*-bis((*1H*-pyrazol-1-yl)methyl)-2-(phenylthio)ethan-1-amine (bpmpe) in presence of PF_6^- or BF_4^- anions. All complexes were well characterized by IR, UV–Vis spectroscopy, elemental analysis, magnetic and EPR spectral data. X-ray crystallography study indicate that [Cu(bdmpe/bpmpe)X]PF_6 complexes are mononuclear in solid state and the tetradentate chelation behavior of the ligand bdmpe or bpmpe with square pyramidal geometry at the copper centers. The nickel(II) complex [Ni(bdmpe)(μ-Cl)]$_2$(Y)$_2$.CH_3CN is binuclear with distorted octahedral geometry and two nickel centers are bridged by double chloride ion. EPR spectra of all copper complexes are recorded in DMF solutions at 77 K and show four hyperfine lines spectra with g_{II} = ~2.260 and $g_{\perp}$= ~2.060. Supramolecular dimeric nature of the complexes **1** and **7** are observed due to short intermolecular interactions. The antimicrobial activity of all complexes were investigated against Gram positive (*Bacillus subtilus, Streptococcus aureus*) and Gram negative (*Escherichia coli, Pseudomonas aeruginosa*) bacterial strain by agar well dilution method and have demonstrated significant antimicrobial activity of the compounds. The studies on the interaction of complexes and DNA by agarose gel electrophoresis method revealed that the complexes can effectively cleave the circular plasmid DNA at very low concentrations.

3(A).1. Introduction

The synthesis, characterization, structure and study of bioactivities of new transition metal complexes are presently attracted an interest area of research in bioinorganic chemistry in order to find alternative therapeutics agent in the place of most active cis-platin because of its side effects in the human body [1-4]. Transition metal complexes are subject of research interest for the development of new chemotherapeutic and antimicrobial drugs because the metal ions have structural diversity and reactivity and can bind with wide range of ligands [5-10]. Among the transition metals, copper is the most preferred as it is biocompatible and can bind and cleave DNA under physiological conditions [11-12]. Nitrogen containing flexible multi dentate organic ligands is important choice for the synthesis of model complexes. Among co-ligands, halide anions are the best as they have different coordination modes of binding and exhibit interesting electronic properties in the complexes [13-16]. Pyrazolyl based heterocycle ligands are important class of ligand because of their interesting flexible donor properties towards transition metal ions [17-19]. Ligand with 'soft' S donors e.g. thioether, thiolates etc are considered as bio-ligand and S-containing chelating ligands have useful application [20-22]. Recently we have synthesized, structurally characterized and studied bioactivities of copper(II) and cobalt(II) complexes with tetradentate heterocyclic N_4-coordinate pyrazolyl based ligand in presence of halide or pseudo halides as co-ligands [23-24]. Now we would like to extend our approach with metal complexes with S-containing another tetradentate heterocycles pyrazolyl based N_3S-donor ligand in presence of halide ions.

In this chapter we report on the synthesis, characterization and structures of binuclear nickel(II) complexes of the type $[Ni(bdmpe)\mu\text{-}Cl]_2(Y)_2.CH_3CN$ and copper (II) complexes of the type [Cu(bdmpe/bpmpe)X]Y [X = Cl^- / Br^- and Y = PF_6^- / BF_4^-, bdmpe = *N*,*N*-bis((3,5-dimethyl-*1H*-pyrazol-1-yl)methyl)-2-(phenylthio)ethan-1-amine or bpmpe = *N*,*N*-bis((*1H*-pyrazol-1-yl)methyl)-2-(phenylthio)ethan-1-amine. The crystal structures of four [Cu(bdmpe/bpmpe)X]PF_6 and $[Ni(bdmpe)\mu\text{-}Cl]_2(PF_6)_2.CH_3CN$ complexes have been solved and their antimicrobial activity and DNA cleavage study was evaluated in detail.

3(A).2. Experimental

3(A).2.1. Materials

All chemicals and solvents were analytical grade reagents and purchased from commercial sources. Acetylacetone, paraformaldehyde, hydrazine hydrate, $CuCl_2.2H_2O$, $CuBr_2.4H_2O$ (Loba, India), $NiCl_2.6H_2O$ (Sisco chem, India), NH_4BF_4 and NH_4PF_6 (Aldrich) were reagent grade and used as received. *N*-(3,5-dimethyl-*1H*-pyrazole-1-yl)methanol and *N*,*N*-bis((3,5-dimethyl-*1H*-pyrazol-1-yl)methyl)-2-(phenylthio)ethan-1-amine (bdmpe) were synthesized as per the published procedures [Chapter 2.2.1.]. Luria bertani, Agar, Agarose (molecular biology grade) Ethidium bromide (Himedia, Mumbai, India), Bromophenol blue (0.25%) were purchased from commercial grade. The bacterial plasmid pBS KS(+) was isolated from *Escherichia coli* strain carrying it, by alkaline lysis method [25]. The ratio of ~1.86 for absorbance at 260 to 280 nm (A260/A280) indicates that the DNA is sufficiently free from protein [26]. The concentration of DNA was determined spectrophotometrically (UV 1601 UV-Visible spectrophotometer, SHIMADZU) at 260 nm using the known molar extinction coefficient value of 6700 M^{-1} cm^{-1} [27]. The DNA was stored at -20°C until used. Visualization of DNA under UV was done using Alpha imager HP System, Alpha innotech.

3(A).2.2. Physical Measurements

^1H NMR spectra were recorded on Bruker NMR AV400 spectrometer in $CDCl_3$. The IR spectra were recorded on a Perkin Elmer FT-IR spectrometer RX1 spectrum using KBr pellets. The micro analyses (C, H and N) were carried out using a Perkin Elmer IA 2400 series elemental analyzer. UV-Vis spectra (1100 - 190 nm) of all complexes were recorded on a JASCO V630 (Spectrophotometer) in CH_3CN solution (10^{-3} M). Solution conductivities were measured in CH_3CN solution (10^{-3} M) using Equip-Tronics conductivity meter (model no. EQ-660A). Room temperature magnetic susceptibilities of powder samples were measured using a Faraday magnetic balance equipped with a Metler UMX 5 balance, OMEGA temperature controller with a field strength of 0.8 T using Hg [Co(SCN)4] as the reference. EPR measurements were performed on a Bruker EMX EPR spectrometer using X-band frequency at liquid nitrogen temperature (77 K).

3(A).2.3. Antimicrobial activity assay

To determine the antimicrobial activity, five complexes with resolved structure viz. **1**, **3**, **5**, **7** and **9** were screened against Gram positive (*Bacillus subtilus, Streptococcus aureus*) and Gram negative (*Escherichia Coli, Pseudomonas aeruginosa*) by agar well diffusion method. Various concentrations of Cu(II) complexes in distilled water were prepared with DMSO not more than 0.1% to assist dissolution. All the compounds were tested in duplicates. The Luria Bertani(LB) agar plates with 4 mm thickness were spread with 100 µl of overnight cultures. Test compounds at different concentrations were added to 5 mm diameter wells made in the agar plates. DMSO at the concentration of 0.1% was used as a negative control and 1 mg/mL of chloramphenicol was used as a positive control for the assay. The plates were incubated at 37˚C for 24 hours and then checked for the appearance of zones of inhibition.

3(A).2.4. Cleavage experiment

The Cu(II) complexes **1**, **3**, **5**, **7** and **9** were studied for their ability to cleave DNA. The copper complexes at various concentration ranging from 10-50 µM along with 5 µM hydrogen peroxide were used to treat 3µM pBS KS(+) plasmid DNA. Plasmid with volume made up with sterile distilled water was taken as an untreated control. Plasmid was also incubated with 5 µM H_2O_2 alone and with 50 µM of the complexes alone, to check their individual effect on the plasmid. After overnight incubation at 37˚C, 5 µl from each reaction was loaded using bromophenol blue loading dye (0.25%) onto 0.8% agarose gel containing ethidium bromide (final 0.5 µg/ml). The gel was observed under UV trans illuminator at 360 nm.

3(A).2.5. Preparation of ligand

3(A).2.5.1. Synthesis of *N,N*-bis((*1H*-pyrazol-1-yl)methyl)-2-(phenylthio)ethan-1-amine (bpmpe)

First, 2-(phenylthio)ethan-1-amine was synthesized from thiophenol as par the reported procedure [28]. In the next step, an acetonitrile solution (25 mL) of (1H-pyrazole-1-yl)methanol (1.0 g, 8 mmol) was added to a stirring solution of 2-(phenylthio)ethan-1-amine (0.685 g, 4 mmol) in same solvent (25 mL). The reaction mixture was stirred for two days at room temperature in closed vessel, finally it was

refluxed for 3 h. Progress of the reaction was monitored by TLC. The solution was dried over Na_2SO_4 and solvent was evaporated under reduced pressure. Light yellow color viscous liquid was obtained.

Yield. 1.29 g (92%). Found C = 61.45, H = 6.19, N = 22.45%, Elemental analysis Calc. for $C_{16}H_{19}N_5S$: C = 61.31, H = 6.11, N = 22.34%. IR (neat) cm^{-1}: ν(C = C), 1583 s; ν(C = C) + ν (C = N)/pz ring, 1511s, 1443 s; ν(C-S), 654 w. ^1H NMR(400 MH_Z, $CDCl_3$, 20 °C). δ/ppm: 7.55 (d, 2H, –CH-/pz ring), 7.50 (d, 2H, –CH-/pz ring), 7.19-7.34 (m, 5H, phenyl ring), 6.23-6.30 (t, 2H, J_{HZ} = 2 Hz, –CH-/pz ring), 5.56 (s, 4H, $-CH_2-$), 2.99 (s, 4H, $-CH_2-CH_2-$).

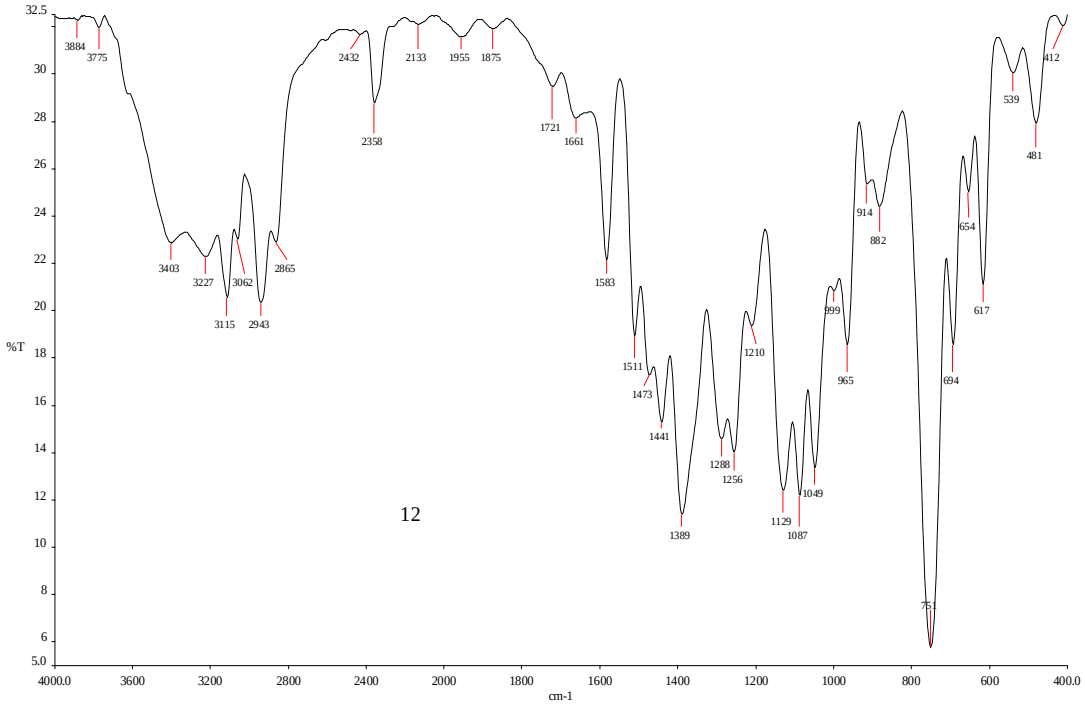

Fig.3(A).1. IR spectrum of *N*,*N*-bis((*1H*-pyrazol-1-yl)methyl)-2-(phenylthio)ethan-1-amine (bpmpe).

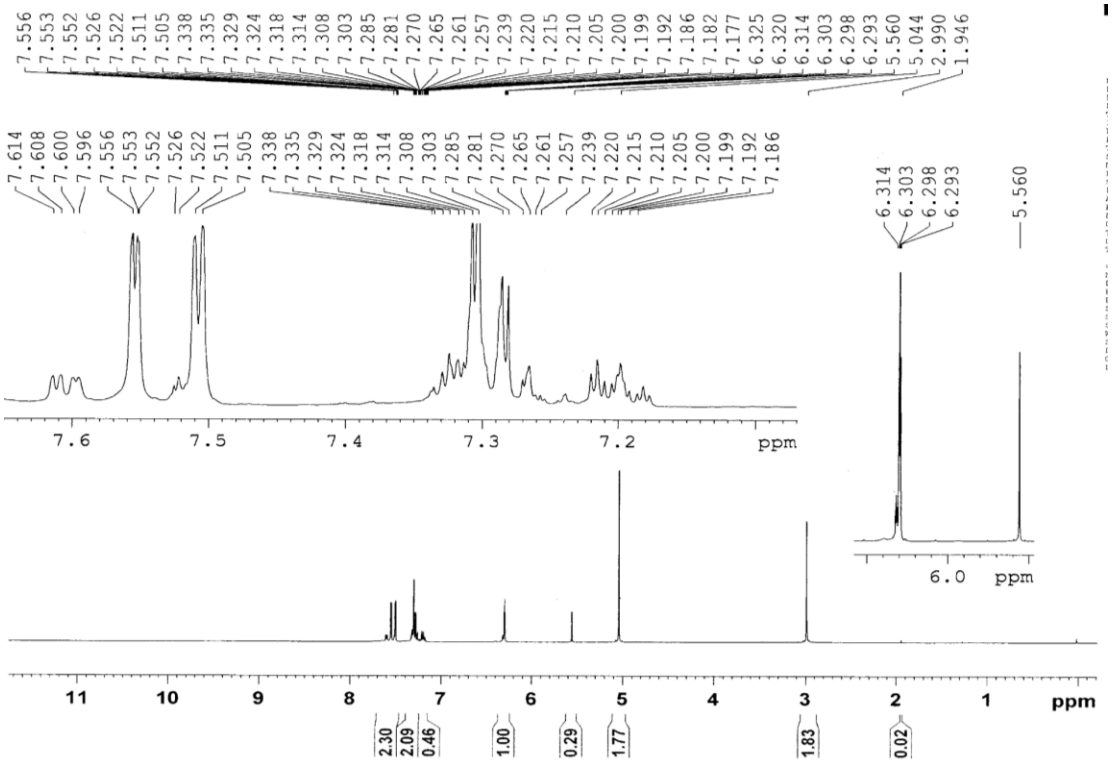

Fig.3(A).2. ^{1}H NMR spectrum of *N*,*N*-bis((*1H*-pyrazol-1-yl)methyl)-2-(phenylthio)ethan-1-amine (bpmpe).

3(A).2.6. Syntheses of the complexes

3(A).2.6.1. Synthesis of [Cu(bdmpe)Cl]PF_6 (1)

Ligand bdmpe (0.185 g, 0.5 mmol) was dissolved in methanol (20 ml) and added drop by drop to a stirring solution of $CuCl_2.2H_2O$ (0.085 g, 0.5 mmol) in the same solvent (10 ml) and the color of the solution changed to dark green immediately. After 10 min, NH_4PF_6 (0.082 g, 0.5 mmol) in methanol (10 ml) was added drop by drop in the mixture and resulting dark green color solution was stirred for another 3 h at ambient temperature and filtered. The filtrate was allowed to evaporate slowly at ambient temperature which gave dark green color single crystals suitable for X-ray diffraction after a week.

Yield. 0.132 g (83%). Found C = 39.54, H = 4.49, N = 11.30%. Anal calc for $C_{20}H_{27}ClCuF_6N_5PS$: C = 39.16, H = 4.44, N = 11.42%. IR (KBr pellet) cm^{-1}: ν(-NH), 3329 vs; ν(C = C)/ph ring, 1600 s; ν(C = C) + ν (C = N)/pz ring 1551 s, 1474 s; ν(PF_6^-), 848 br. UV-Vis spectra: λ_{max}/nm (ε_{max}/$mol^{-1}cm^{-1}$). 663 (189), 285 (5842), 249 (14182), 224 (24672). Λ_M ($\Omega^{-1}cm^2\,mol^{-1}$) = 120. μ_{eff} = 1.76 BM.

3(A).2.6.2. Synthesis of [Cu(bdmpe)Cl]BF_4 (2)

This complex was prepared by following the same procedure as that of complex **1**, except NH_4BF_6 was used in the place of NH_4PF_6.

Yield. 0.110 g (79%). Found C = 43.65 , H = 4.93 , N = 12.43%, Anal calc for $C_{20}H_{27}BClCuF_4N_5S$: C = 43.26, H = 4.90, N = 12.61%. IR (KBr pellet) cm^{-1}: ν(-NH), 3132 vs; ν(C = C)/ph ring, 1600 s; ν(C = C) + ν (C = N)/pz ring, 1555 s, 1476 s; ν(BF_4^-), 1055 br. UV-Vis spectra: λ_{max}/nm (ε_{max}/$mol^{-1}cm^{-1}$). 667 (158), 283 (4509), 247 (11180), 222 (20577). Λ_M ($\Omega^{-1}cm^2\,mol^{-1}$) = 120. μ_{eff} = 1.72 BM.

3(A).2.6.3. Synthesis of [Cu(bdmpe)Br]PF_6 (3)

This complex was prepared by following the same procedure as that of complex **1**, except $CuBr_2.2H_2O$ was used instead of $CuCl_2.2H_2O$.

Yield. 0.129 g (78%). Found C = 36.15, H = 4.17, N = 10.76%. Anal calc for $C_{20}H_{27}BrCuF_6N_5PS$: C = 36.51, H = 4.14, N = 10.64%. IR (KBr pellet) cm^{-1}: ν(-NH), 3242 vs; ν(C = C)/ph ring, 1603 s; ν(C = C) + ν (C = N)/pz ring 1558 s, 1476 s, ν(PF_6^-), 839 s. UV-Vis spectra: λ_{max}/nm (ε_{max}/$mol^{-1}cm^{-1}$). 667 (268), 315 (3572), 249 (9325), 223 (19676). Λ_M ($\Omega^{-1}cm^2\,mol^{-1}$) = 120. μ_{eff} = 1.78 BM.

3(A).2.6.4. Synthesis of [Cu(bdmpe)Br]BF_4 (4)

This complex was prepared by following the same procedure as that of complex **1**, except $CuBr_2.2H_2O$ and NH_4BF_4 was used instead of $CuCl_2.2H_2O$ and NH_4PF_6.

Yield. 0.120 g (73%). Found C = 40.42, H = 4.56, N = 11.44%. Anal calc for $C_{20}H_{27}BBrCuF_4N_5S$: C = 40.05, H = 4.54, N = 11.68%. IR (KBr pellet) cm^{-1}: ν(-NH), 3326 vs; ν(C = C)/ph ring, 1633 s; ν(C = C) + ν (C = N)/pz ring 1553 s, 1470 s; ν(BF_4^-), 1042 br. UV-Vis spectra: λ_{max}/nm (ε_{max}/$mol^{-1}cm^{-1}$). 673 (268), 314 (3497), 248 (9129), 221 (20469). Λ_M ($\Omega^{-1}cm^2\,mol^{-1}$) = 120. μ_{eff} = 1.77 BM.

3(A).2.6.5. Synthesis of [Cu(bpmpe)Cl]PF_6 (5)

This complex was prepared by following the same procedure as that of complex **1**, except ligand bpmpe was used instead of ligand bdmpe.

Yield. 0.113 g (81%). Found C = 34.88, H = 3.39, N = 12.73%. Anal calc for $C_{16}H_{19}ClCuF_6N_5PS$: C = 34.48, H = 3.44, N = 12.56%. IR (KBr pellet) cm^{-1}: ν(-NH), 3329 vs; ν(C = C)/ph ring, 1600 s; ν(C = C) + ν (C = N)/pz ring 1551 s, 1474 s; ν(PF_6^-), 848 s. UV-Vis spectra: λ_{max}/nm (ε_{max}/$mol^{-1}cm^{-1}$). 749 (102), 283 (4635), 248 (9069). Λ_M ($\Omega^{-1}cm^2\ mol^{-1}$) = 120. μ_{eff} = 1.74 BM.

3(A).2.6.6. Synthesis of [Cu(bpmpe)Cl]BF_4 (6)

This complex was prepared by following the same procedure as that of complex **1**, except ligand bpmpe and NH_4BF_6 were used instead of ligand bdmpe and NH_4PF_6.

Yield. 0.099 g (79%). Found C = 38.96 , H = 3.80 , N = 14.11%, Anal calc for $C_{16}H_{19}BClCuF_4N_5S$: C = 38.50, H = 3.84, N = 14.03%. IR (KBr pellet) cm^{-1}: ν(-NH), 3132 vs; ν(C = C)/ph ring, 1600 s; ν(C = C) + ν (C = N)/pz ring, 1555 s, 1476 s; ν(BF_4^-), 1055 br. UV-Vis spectra: λ_{max}/nm (ε_{max}/$mol^{-1}cm^{-1}$). 706 (103), 284 (4745), 247 (10294). Λ_M ($\Omega^{-1}cm^2\ mol^{-1}$) = 120. μ_{eff} = 1.76 BM.

3(A).2.6.7. Synthesis of [Cu(bpmpe)Br]PF_6 (7)

This complex was prepared by following the same procedure as that of complex **1**, except ligand bpmpe and $CuBr_2.2H_2O$ were used instead of ligand bdmpe and $CuCl_2.2H_2O$.

Yield. 0.114 g (76%). Found C = 32.12, H = 3.14, N = 11.56%. Anal calc for $C_{16}H_{19}BrCuF_6N_5PS$: C = 31.93, H = 3.18, N = 11.64%. IR (KBr pellet) cm^{-1}: ν(-NH), 3242 vs; ν(C = C)/ph ring, 1603 s; ν(C = C) + ν (C = N)/pz ring 1558 s, 1476 s, ν(PF_6^-), 839 s. UV-Vis spectra: λ_{max}/nm (ε_{max}/$mol^{-1}cm^{-1}$). 670 (139), 318 (4298), 248 (8889). Λ_M ($\Omega^{-1}cm^2\ mol^{-1}$) = 120. μ_{eff} = 1.75 BM.

3(A).2.6.8. Synthesis of [Cu(bpmpe)Br]BF_4 (8)

This complex was prepared by following the same procedure as that of complex **1**, except $CuBr_2.2H_2O$, ligand bpmpe and NH_4BF_4 was used instead of $CuCl_2.2H_2O$, ligand bdmpe and NH_4PF_6.

Yield. 0.107 g (79%). Found C = 35.21, H = 3.55, N = 12.76%. Anal calc for $C_{16}H_{19}BBrCuF_4N_5S$: C = 35.35, H = 3.52, N = 12.88%. IR (KBr pellet) cm^{-1}: ν(-NH), 3326 vs;ν(C = C)/ph ring, 1633 s; ν(C = C) + ν (C = N)/pz ring 1553 s, 1470 s;

$\nu(BF_4^-)$, 1042 br. UV-Vis spectra: λ_{max}/nm (ε_{max}/$mol^{-1}cm^{-1}$). 663 (225), 315 (5712), 248 (10915). Λ_M ($\Omega^{-1}cm^2\ mol^{-1}$) = 120. μ_{eff} = 1.76

3(A).2.6.9. Synthesis of $[Ni(bdmpe)Cl]_2(PF_6)_2$ (9)

A colorless solution of ligand bdmpe (0.185 g, 0.5 mmol) in methanol (10-20 ml) was added slowly to a stirred solution of nickel(II) chloride hexahydrate (0.119 g, 0.5 mmol) in methanol (10 ml) at room temperature and the solution immediately turned bright green. Then, methanol solution of NH_4PF_6 (0.082 g, 0.5 mmol) was drop by drop added to the reaction mixture, resulting solution was stirred for another 3 h at room temperature and filtered. The filtrate was allowed to evaporate slowly at ambient temperature. After one week light green color powder compound was isolated by filtration. Small amount of compound was dissolved in acetonitrile and kept for slow evaporation. Light green color single crystals suitable for X-ray diffraction were obtained after five days

Yield. 0.081 g (52%). Found C = 40.44, H = 4.52, N = 12.42%. Anal calc for $C_{40}H_{54}Cl_2Ni_2F_{12}N_{10}P_2S_2$: C = 40.09, H = 4.57, N = 12.24%. IR (KBr Pellet) cm^{-1}: ν(-NH), 3197 vs; ν(C = C)/ph ring, 1603 s; ν(C = C) + ν (C = N)/pz ring 1556 s, 1476 s; $\nu(PF_6^-)$, 840 s. UV-Vis spectra: λ_{max}/nm (ε_{max}/$mol^{-1}cm^{-1}$). 830 (54), 628 (207), 607 (349), 531 (234), 501 (271), 245 (17259), 200 (32821). Λ_M ($\Omega^{-1}cm^2\ mol^{-1}$) = 120. μ_{eff} = 2.89

3(A).2.6.10. Synthesis of $[Ni(bdmpe)Cl]_2(BF_4)_2$ (10)

This complex was prepared by following the same procedure as that of complex **9**, except NH_4BF_6 was used instead of NH_4PF_6.

Yield. 0.088 g (55%). Found C = 44.42, H = 5.08, N = 13.64%. Anal calc for $C_{40}H_{54}Cl_2Ni_2F_8N_{10}B_2S_2$: C = 44.17, H = 5.03, N = 13.49%. IR (KBr pellet) cm^{-1}: ν(-NH), 3197 vs; ν(C = C)/ph ring, 1603 s; ν(C = C) + ν (C = N)/pz ring, 1556 s, 1476 s; $\nu(PF_6^-)$, 840 s. UV-Vis spectra: λ_{max}/nm (ε_{max}/$mol^{-1}cm^{-1}$). 829 (33), 632 (109), 605 (274), 530 (182), 501 (201), 290 (5669), 246 (26217). Λ_M ($\Omega^{-1}cm^2\ mol^{-1}$) = 122. μ_{eff} = 2.88.

3(A).3. X-ray Crystallography

The summary of data collection and structure refinement parameters for the complexes **1, 3, 5, 7** and **9** are given in Table 3(A).1 and selected bond lengths (Å) and angels (º) are given in Table 3(A).2. Suitable single crystals were placed in viscous oil, carefully selected under a polarizing microscope and mounted on a glass fiber. Accurate unit cell parameters were determined by a least squares fit of 2θ values and reflection intensity data collection which performed on Oxford X-CALIBUR-S diffractometer equipped with Cu-Kα radiation (λ = 1.54184 Å) for all copper complexes **1**, **3**, **5** and **7** whereas for complex **9**, graphite-monochromator Mo-Kα radiation (λ = 0.71073 Å) were used at 110 K. The data interpretations were processed with CrysAlisPro, Agilent Technologies, Version 1.171.35.19 [29]. An absorption correction based on multi-scan method was applied [30]. All structures were solved by direct method and refined by the full-matrix least-square based on F^2 technique using SHELXL-97 program package [31]. At convergence, the final residual were R1 = 0.0392 (for complex **1**), 0.1498 (for complex **3**), 0.0796 (for complex **5**), 0.0509 (for complex **7**) and 0.0502 (for complex **9**); R2 = 0.0998 (for complex **1**), 0.4143 (for complex 3), 0.2152 (for complex **5**), 0.1255 (for complex **7**) and 0.1254 (for complex **9**) with I >2σ (I), goodness fit = 1.050 (for complex **1**), 1.711 (for complex **3**), 1.046 (for complex **5**), 1.042 (for complex **7**) and 0.786 (for complex **9**). The final differences Fourier map showed the maximum and minimum peak heights of 0.51 and -0.45 eA^{-3} for **1**, 3.06 and -2.22 eA^{-3} for **3**, 1.25 and -1.58 eA^{-3} for **5**, 1.05 and -0.91 eA^{-3} for **7** and 1.38 and -0.80 eA^{-3} for **9**. All calculations were carried out using WinGX system Ver-1.64 [32]. All non-hydrogen atoms were refined anisotropically. The positions of the hydrogen atoms were located in their calculated position and treated as riding on the atoms to which they are attached. The positions of the hydrogen atoms were calculated from the difference Fourier map, placed in the calculated positions and constrained to ride on their parent atoms. ORTEP3 for Windows program were used for generating for molecular graphics [33].

Table 3(A).1. Crystallographic data for complexes **1**, **3**, **5**, **7** and **9.**

Empirical formula	$C_{20}H_{27}N_5F_6PSClCu$ **(1)**	$C_{20}H_{27}N_5SCuBrPF_6$ **(3)**	$C_{16}H_{19}N_5F_6PSClCu$ **(5)**	$C_{16}H_{19}N_5F_6PSBrCu$ **(7)**	$C_{22}H_{30}ClF_6N_6NiPS$ **(9)**
Formula weight	613.48	657.94	557.38	601.84	1299.38
Temperature (K)	110(2)	110(2)	110(2)	110(9)	110(16)
Wavelength (Å)	CuKα (λ = 1.54184)	CuKα (λ = 1.54184)	CuKα (λ = 1.54184)	CuKα (λ = 1.54184)	Mo Kα (λ = 0.71073)
Crystal system	triclinic	triclinic	monoclinic	Monoclinic	triclinic
Space group	*P-1*	*P-1*	$P2_1/n$	$P2_1/n$	*P-1*
a (Å)	10.4204(3)	10.6527(8)	12.7283(4)	12.7321(5)	11.0249(4)
b (Å)	11.0609(3)	11.4895(7)	14.5278(4)	14.7070(4)	11.4722(4)
c (Å)	12.1143(4)	11.8376(10)	13.2624(4)	13.1689(5)	12.8399(4)
α, (°)	77.218(3)	99.044(6)	90	90	109.352(3)
β(°)	69.251(3)	107.401(7)	115.443(4)	113.876(4)	103.349(3)
γ (°)	86.571(2)	105.308(6)	90	90	105.341(3)
Volume ($Å^3$)	1273.10(7)	1288.85(18)	2214.55(13)	2254.87(15)	1384.13(10)
Z	2	2	4	4	2
Density (g cm^{-3})	1.600	1.695	1.672	1.773	1.559
Absorption coefficient (mm^{-1})	4.120	4.933	4.672	5.574	0.995
F(000)	626.0	659.9	1124.0	1196.0	668.0

θ range for data collection (°)	8.198 to 146.306	8.098 to 152.806	9.57 to 144.464	9.492 to 146.446	6.32 to 58.1
Index ranges	$-12 \le h \le 12$, $-9 \le k \le 13$, $-14 \le l \le 15$	$-12 \le h \le 13$, $-14 \le k \le 11$, $-14 \le l \le 12$	$-15 \le h \le 7$, $-15 \le k \le 17$, $-15 \le l \le 16$	$-15 \le h \le 14$, $-17 \le k \le 18$, $-16 \le l \le 16$	$-14 \le h \le 15$, $-15 \le k \le 15$, $-17 \le l \le 17$
Reflections collected	12114	8453	8786	13143	29823
Independent reflections	5098 [R_{int} = 0.0311]	5412 [R_{int} = 0.0797]	4371 [R_{int} = 0.0499]	4520 [R_{int} = 0.0356]	7393 [R_{int} = 0.0346]
Data / restraints / parameters	5098/0/316	5411/0/319	4371/0/280	4520/0/280	7393/0/347
Goodness-of-fit on F^2	1.050	1.711	1.046	1.042	0.786
Final R indices [I>2sigma(I)]	R_1 = 0.0365, wR_2 = 0.0971	R_1 = 0.1371, wR_2 = 0.3860	R_1 = 0.0732, wR_2 = 0.2023	R_1 = 0.0467, wR_2 = 0.1215	R_1 = 0.0445, wR_2 = 0.1194
R indices (all data)	R_1 = 0.0392, wR_2 = 0.0998	R_1 = 0.1498, wR_2 = 0.4143	R_1 = 0.0796, wR_2 = 0.2152	R_1 = 0.0509, wR_2 = 0.1255	R_1 = 0.0502, wR_2 = 0.1254
Largest diff. peak and hole (eA^{-3})	0.51 and -0.45	3.06 and -2.22	1.25 and -1.58	1.05 and-0.91	1.38 and -0.80
CCDC number	1543129	1543119	1543130	1543131	1565635

3(A).4. Results and Discussion

3(A).4.1. Syntheses

In the present work we describe synthesis of a pyrazole appended tetradentate N_3S-ligand and discuss its binding behavior with metal halides. The ligands *N*,*N*-bis((3, 5-dimethyl-1H-pyrazol-1-yl)methyl)-2-(phenylthio)ethan-1-amine (bdmpe) and *N*,*N*-bis((1H-pyrazol-1-yl)methyl)-2-(phenylthio)ethan-1-amine (bpmpe) were synthesized as viscous yellow liquid by [1+2] condensation of 2-(phenylthio)ethan-1-amine and 3, 5-dimethylpyrazol-1-methanol or (1H-pyrazol-1-yl)methanol using acetonitrile at room temperature for three days **[**Scheme 3(A).1**]** and characterized by IR and ^{1}H NMR spectra. Both ligands possess four potential donor sites- two nitrogen donor atoms from the two pyrazole rings, one nitrogen atom from the tertiary amine and one sulfur atom from the aryl sulphur.

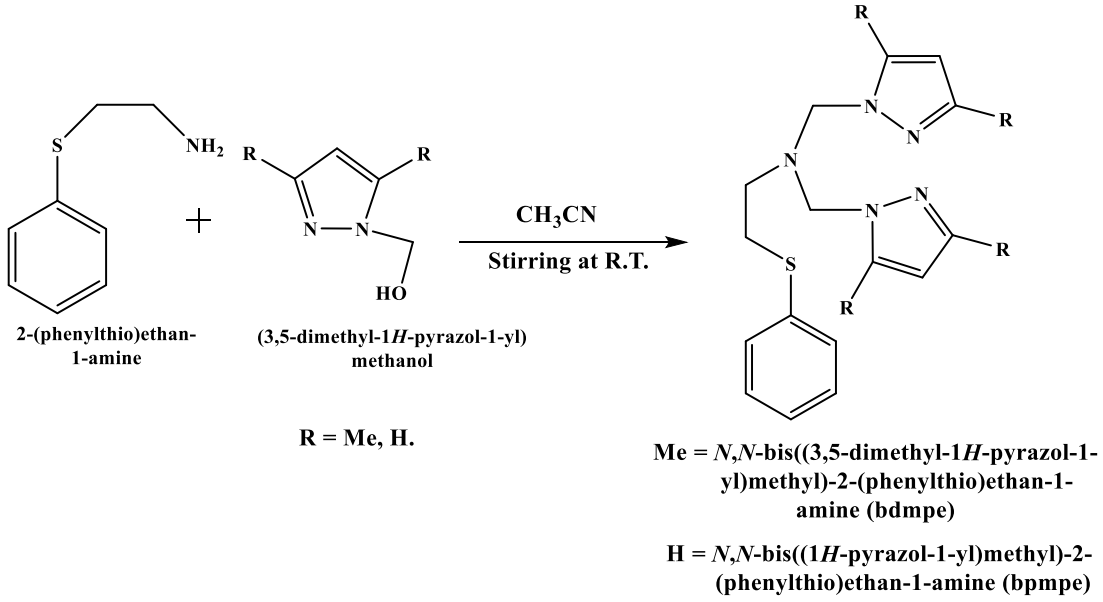

Scheme 3(A).1. Synthesis of ligands.

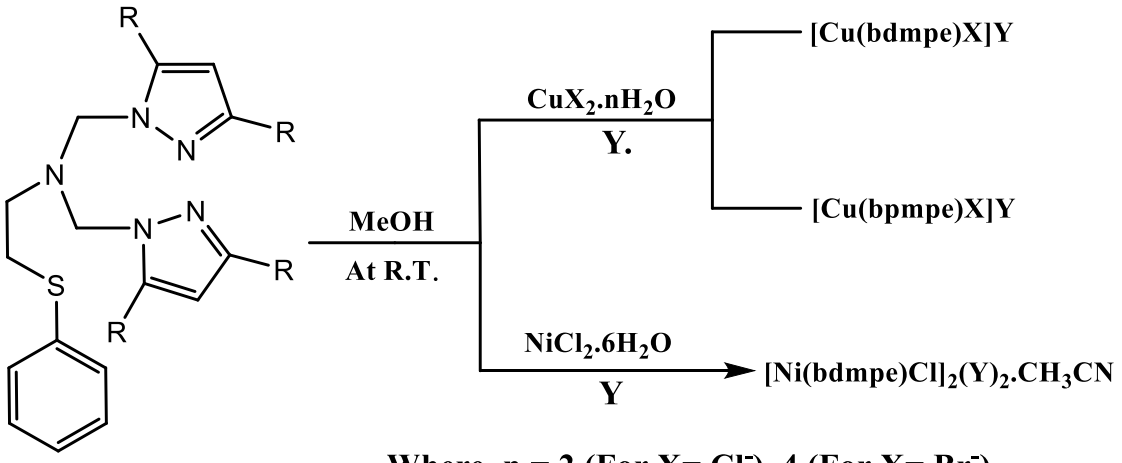

R= Me, H.

Where, n = 2 (For X= Cl^-), 4 (For X= Br^-)

Y = PF_6^-, BF_4^-.

[Cu(bdmpe)Cl]PF_6 (1) and [Cu(bdmpe)Cl]BF_4 (2)

[Cu(bdmpe)Br]PF_6 (3) and [Cu(bdmpe)Br]BF_4 (4)

[Cu(bpmpe)Cl]PF_6 (5) and [Cu(bpmpe)Cl]BF_4 (6)

[Cu(bpmpe)Br]PF_6 (7) and [Cu(bpmpe)Br]BF_4 (8)

[Ni(bdmpe)Cl]$_2$(PF_6)$_2$.CH_3CN (9) and [Ni(bdmpe)Cl]$_2$(BF_4)$_2$.CH_3CN (10)

Scheme 3(A).2. Synthesis of complexes.

Five coordinated eight mononuclear copper(II) complexes [Cu(bdmpe/bpmpe)X]Y[X = Cl^-/ Br^- and Y = PF_6^- / BF_4^-] and six coordinated two binuclear nickle(II) complexes [Ni(bdmpe)(μ-Cl)]$_2$(Y)$_2$.CH_3CN (**9-10**) [where, Y = PF_6^-, BF_4^-] have been obtained with good yield by reacting the appropriate metal salt, corresponding ligand bdmpe/bpmpe and NH_4PF_6/NH_4BF_4 in ratio of 1:1:1 in methanol at room temperature [scheme 3(A).2]. The molecular composition of the complexes were confirmed by microanalysis, IR, molar conductance and UV-Vis spectroscopy data. The molar conductivity measurements in 10^{-3} M CH_3CN solutions revealed the formation of 1:1 electrolyte complexes and indicate the presence of counter anion in the molecules [34]. There was no change in molar conductivity even after 2 h, indicating no change of molecular composition of the complexes in the solution. Further the presence of counter anion was also confirmed by single crystal X-ray diffraction studies. All synthesized complexes are insoluble in water but soluble in common polar organic solvents like methanol, ethanol, acetone and CH_3CN.

3(A).4.2. IR Spectral data

IR spectra of ligands and complexes showing many characteristics bands with possible assignments are reported in section 3(A).2.6. The IR spectrum of ligand bpmpe / bdmpe has shown a sharp intense band at ~ 1583 cm^{-1} assigned as *ν*(C=C) of phenyl ring, at ~ 1553 and ~ 1467 cm^{-1} due to vibration of *ν*(C=N) + *ν*(C=C) of the pyrazole ring. The bands are also present in the all complexes indicating the coordination of ligand bpmpe / bdmpe with respective metal center. Complexes **1**, **3, 5, 7** and **9** show an intense band at ~845 cm^{-1} confirming the presence of ν(PF_6^-) counter anion and complexes **2**, **4**, **6, 8** and **10** exhibited a broad band at ~1065 cm^{-1} indicating the presence of ν(BF_4^-) counter anion outside the coordination sphere [35].

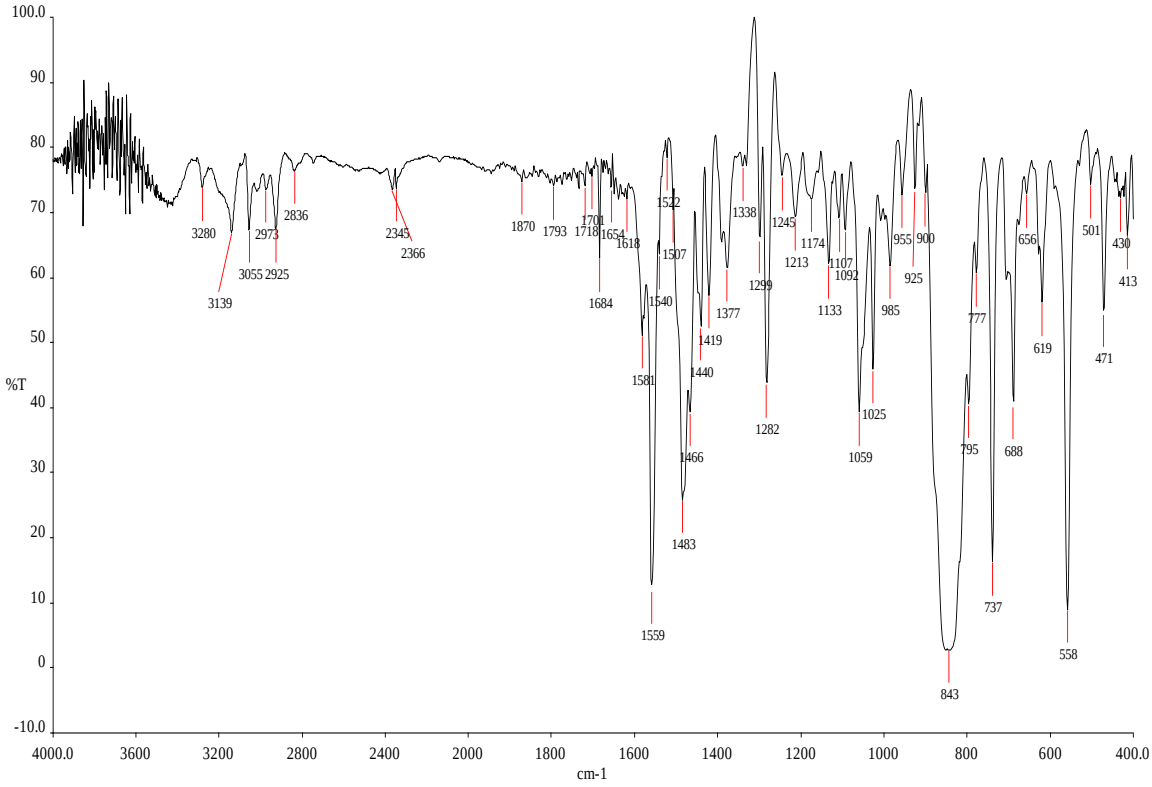

Fig.3(A).3. IR spectrum of [Cu(bdmpe)Cl]PF_6 (**1**).

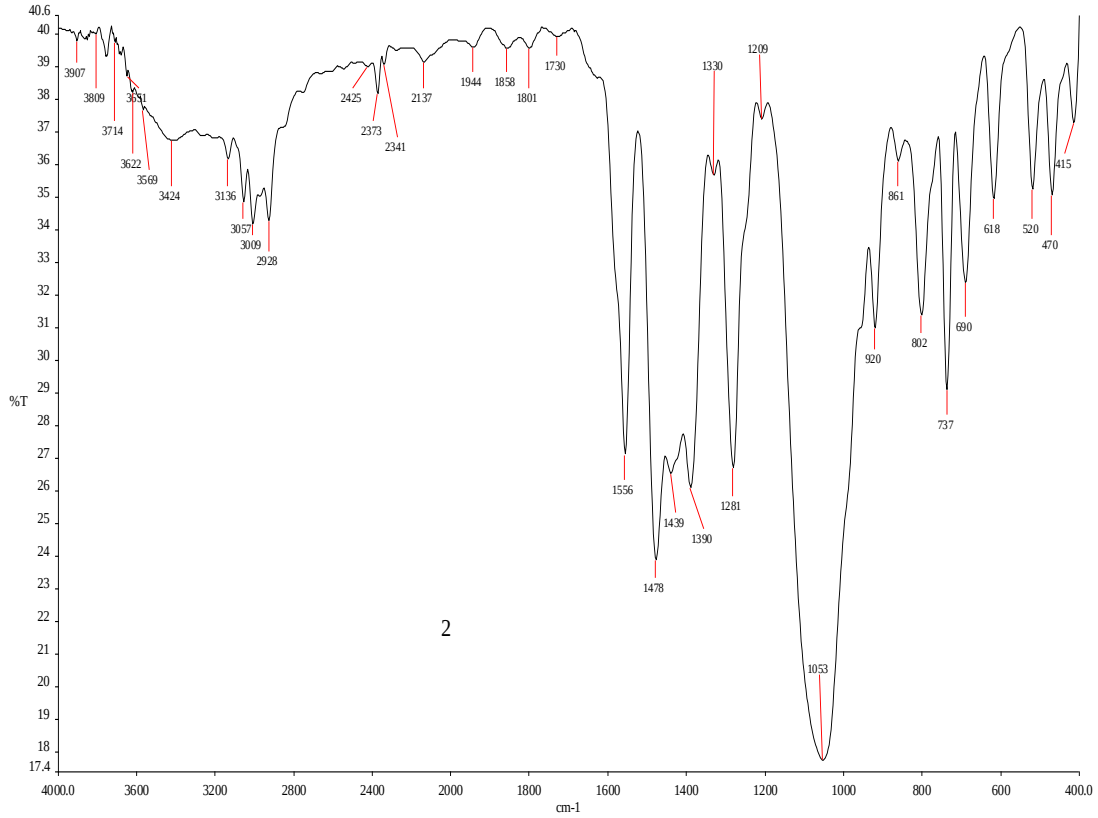

Fig.3(A).4. IR spectrum of [Cu(bdmpe)Cl]BF_4 (**2**).

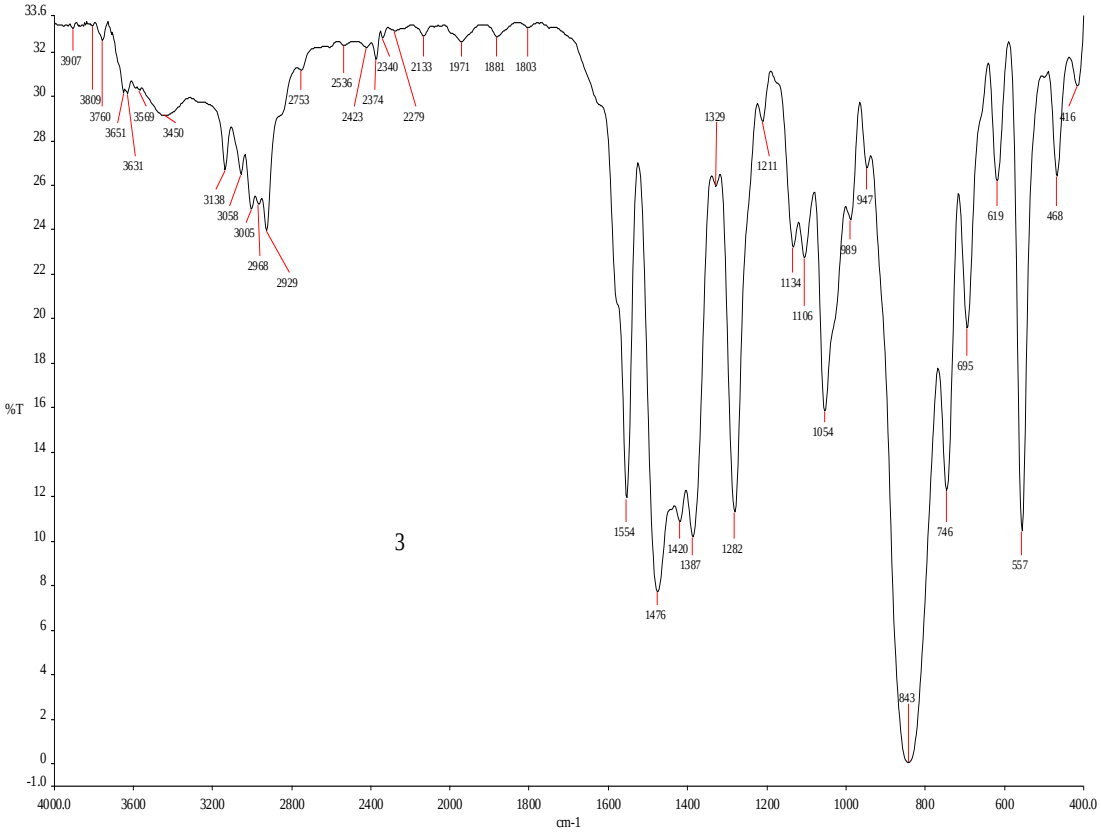

Fig.3(A).5. IR spectrum of [Cu(bdmpe)Br]PF_6 (**3**).

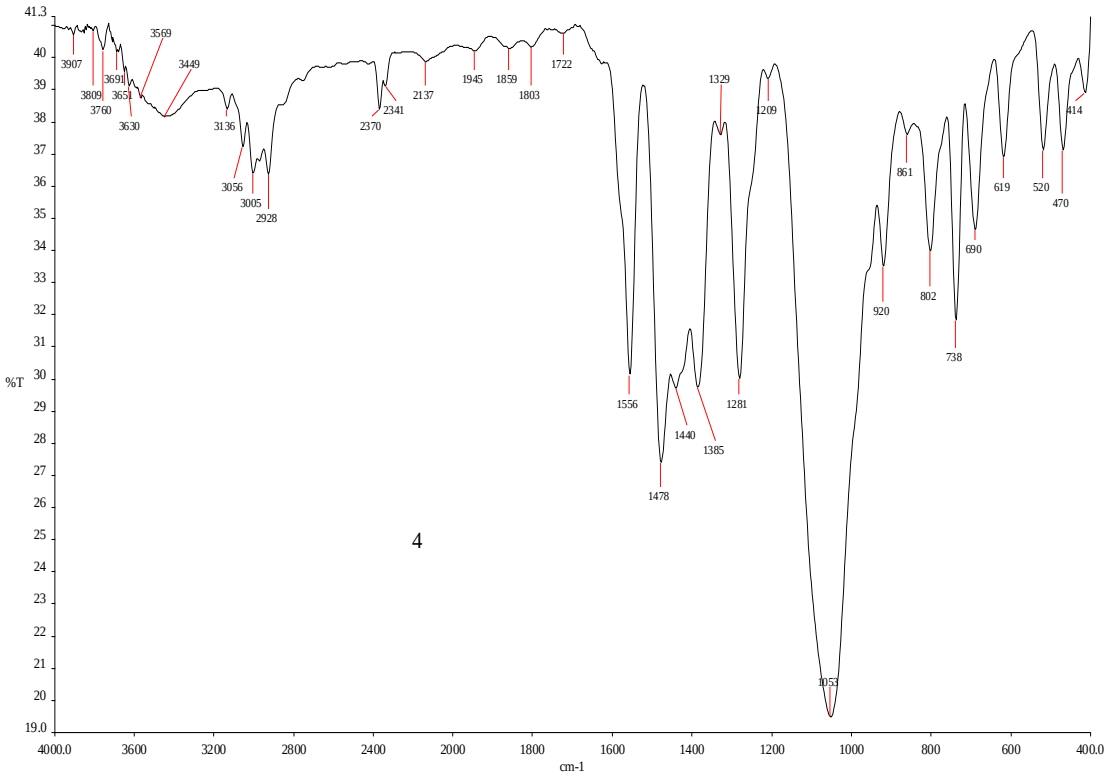

Fig.3(A).6. IR spectrum of [Cu(bdmpe)Br]BF_4 (**4**).

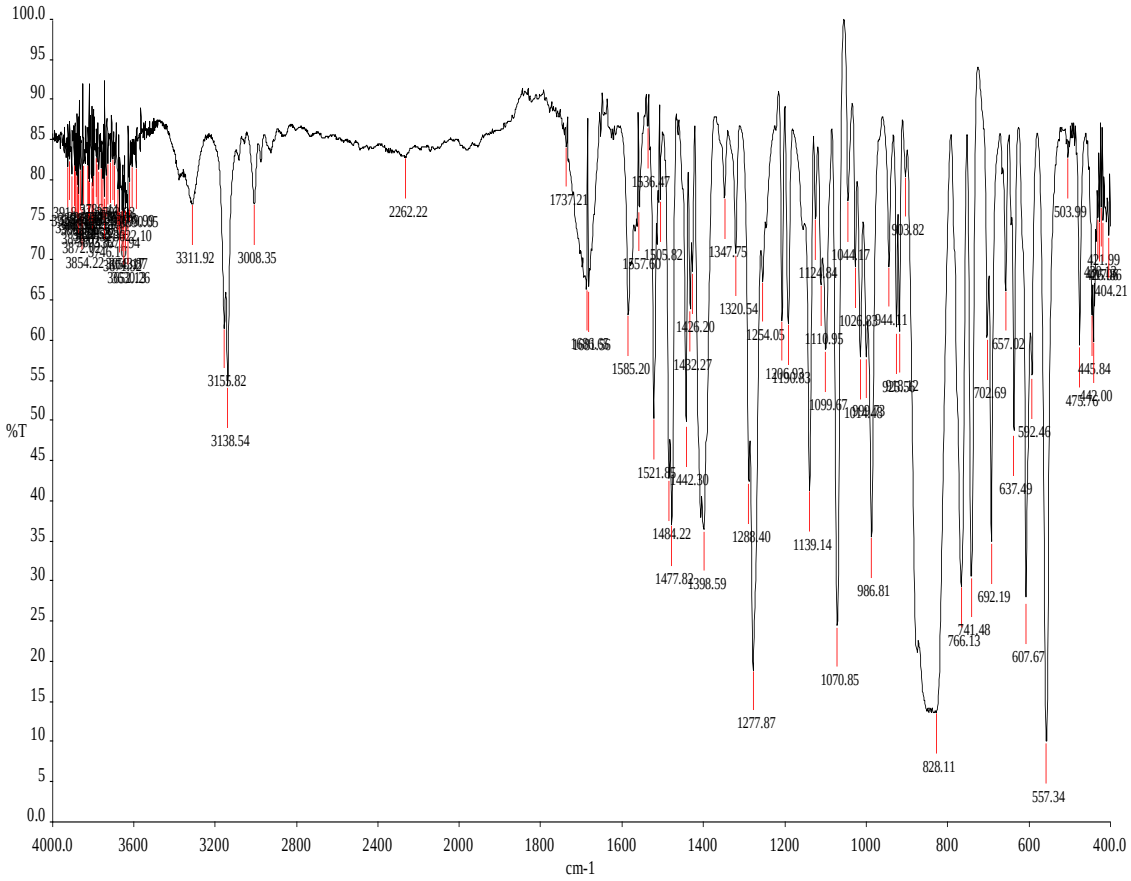

Fig.3(A).7. IR spectrum of [Cu(bpmpe)Cl]PF_6 (**5**).

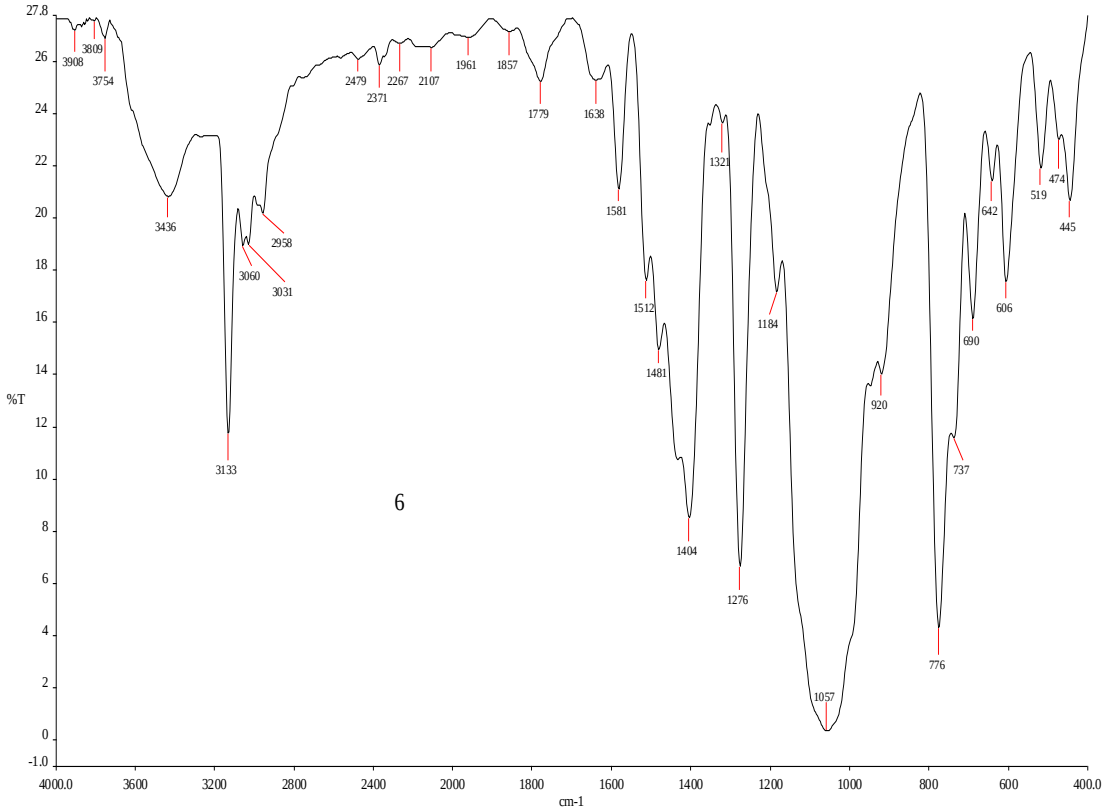

Fig.3(A).8. IR spectrum of [Cu(bpmpe)Cl]BF_4 (**6**).

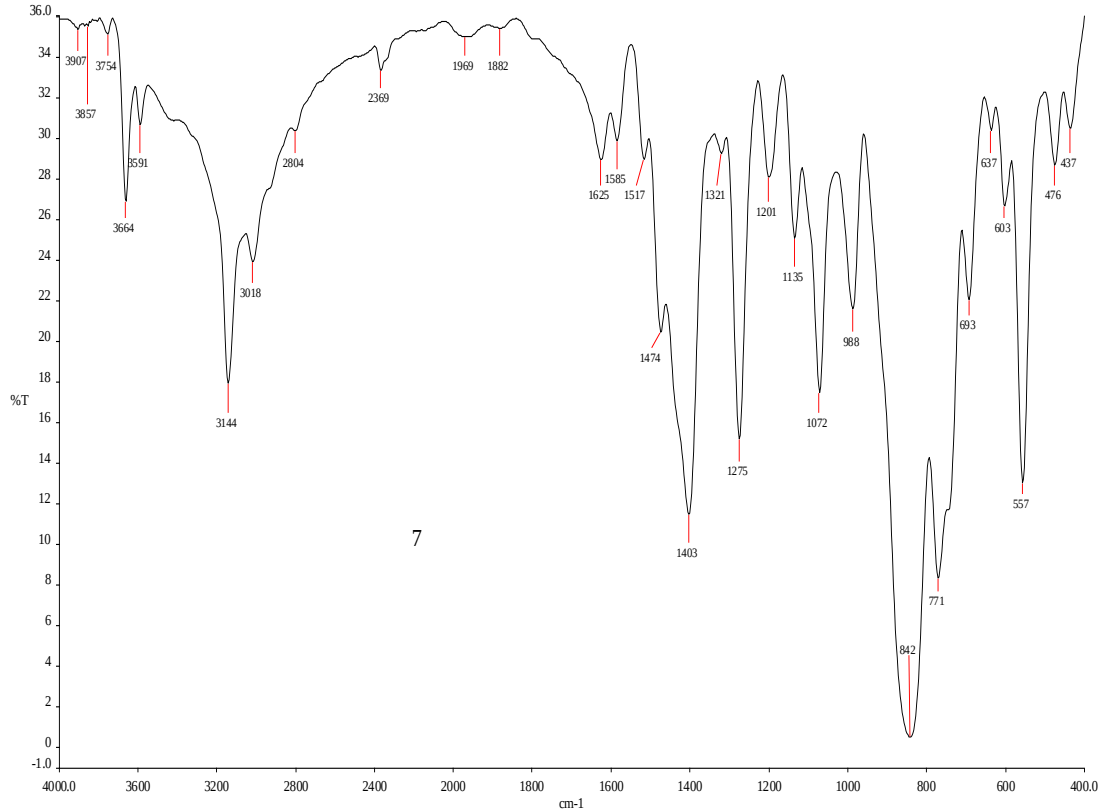

Fig.3(A).9. IR spectrum of [Cu(bpmpe)Br]PF_6 (**7**).

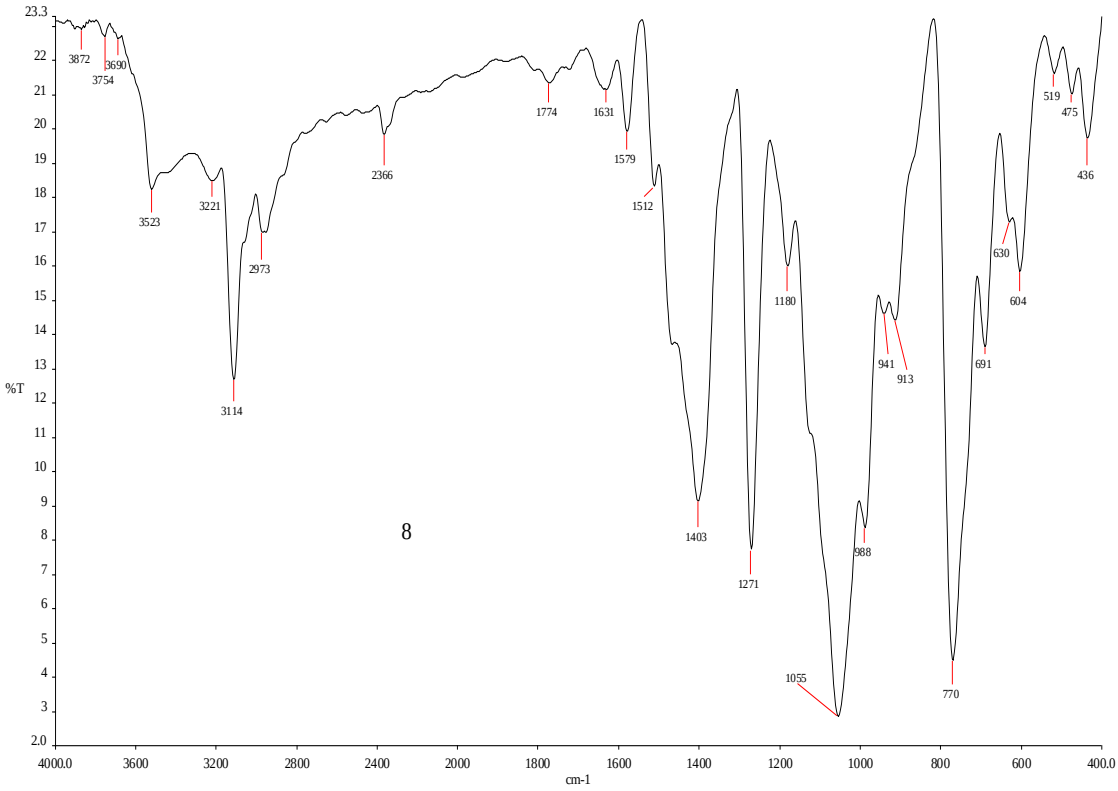

Fig.3(A).10. IR spectrum of [Cu(bpmpe)Br]BF_4 (**8**).

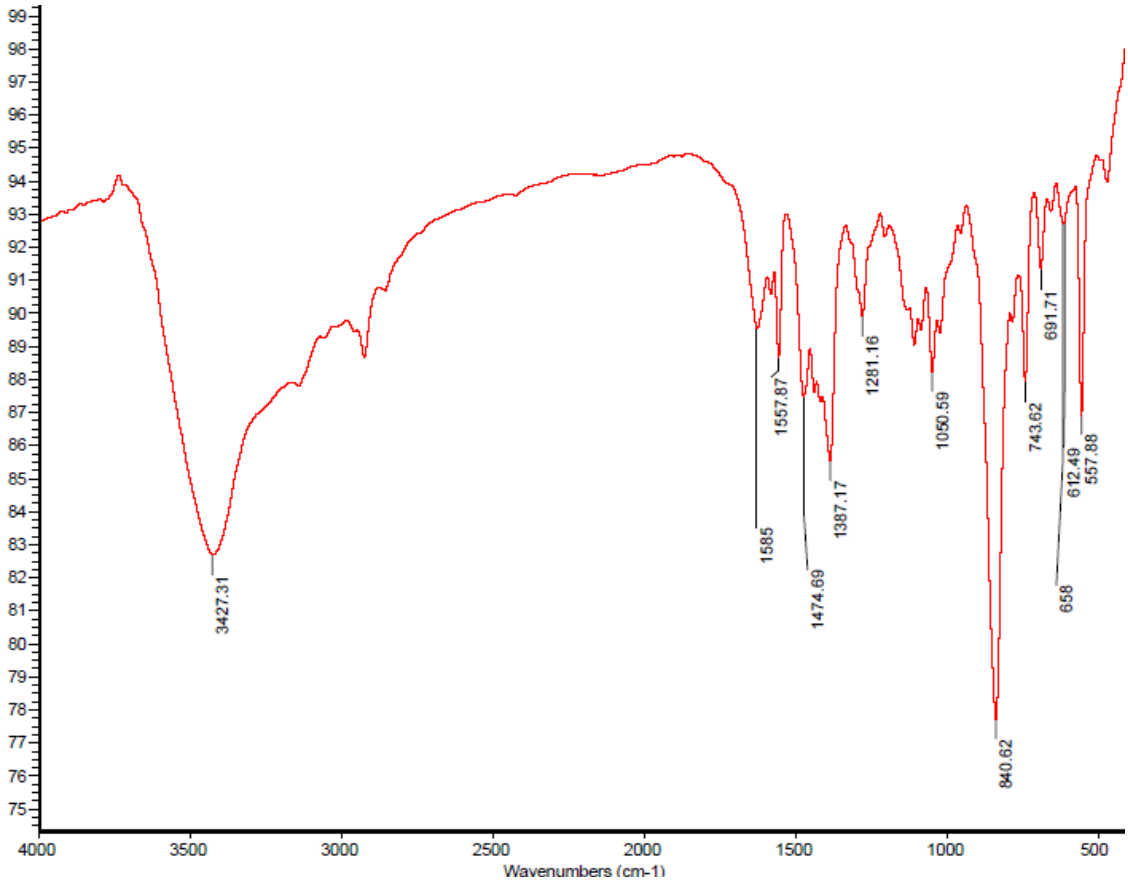

Fig.3(A).11. IR spectrum of $[Ni(bdmpe)Cl]_2(PF_6)_2$ (**9**).

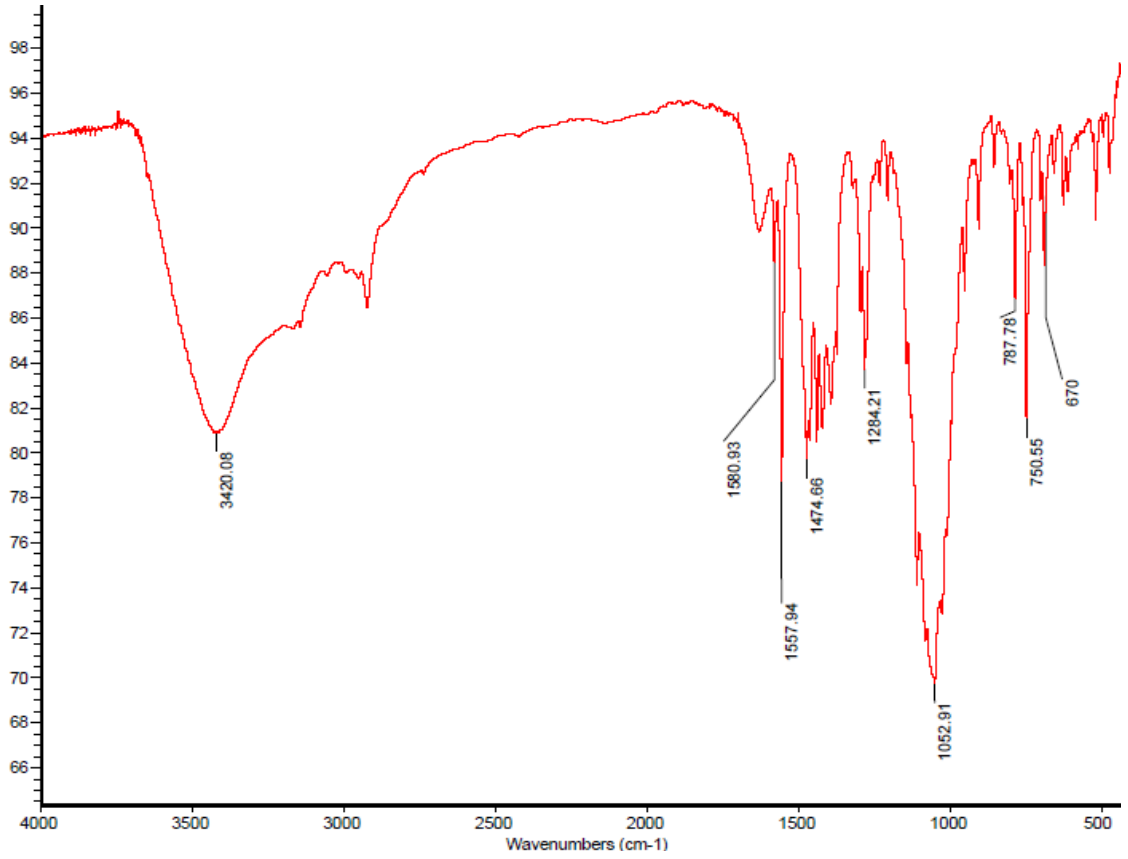

Fig.3(A).12. IR spectrum of $[Ni(bdmpe)Cl]_2(BF_4)_2$ (**10**).

3(A).4.3. UV-Visible spectra, EPR and magnetic data.

The UV-Visible spectral behavior of all the complexes **1-10** were investigated in CH_3CN (10^{-3} M) in the range of 1100-200 nm. The high intensity bands appeared in the 200-400 nm region are due to n-π* and π-π* ligand based charge transfer transition. Generally, Cu(II) complexes with trigonal bipyramidal or distorted trigonal bipyramidal geometry show two spectral bands - one in the region of 700 -750 nm (due to d_{xy}, $d_{yz} \rightarrow d_z^2$) and another at 800-870 nm (due to d_{xy}, $d_x^2-y^2 \rightarrow d_z^2$) transition whereas square pyramidal or distorted square pyramidal Cu(II) complexes show one spectral band in the region of 550 - 670 nm (due to d_{xz}, $d_{yz} \rightarrow d_x^2-y^2$ transition). All copper(II) complexes show a broad absorption band at ~670 nm indicating all complexes have square pyramidal geometry [36-38]. Nickel(II) complexes show two absorption bands at ~1070 and ~ 635 nm with low molar absorption coefficient and these are attributed to d-d transitions or MLCT transition.

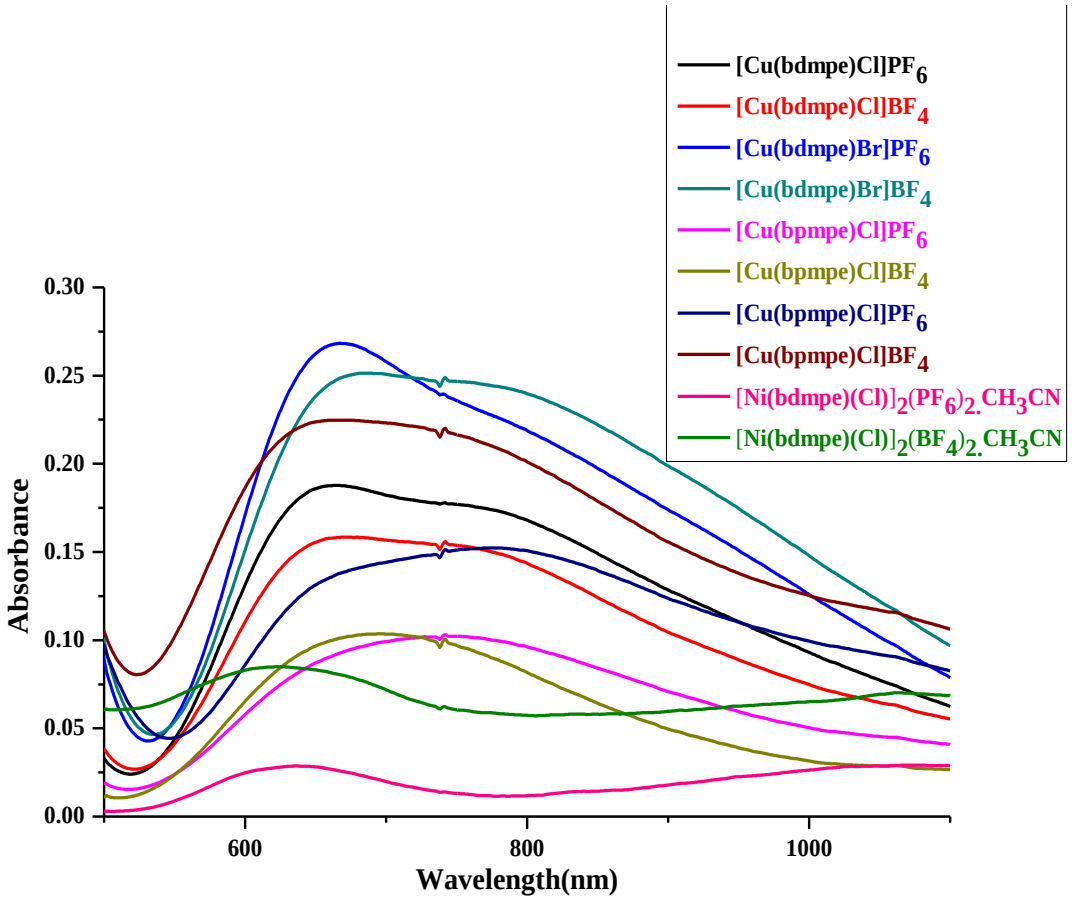

Fig.3(A).13. Electronic spectra of complexes (**1-10**) in CH_3CN (10^{-3} M).

The X-band EPR spectra of the complexes **1**, **3, 5** and **7** in acetonitrile solution (78 K) show four-line splitting pattern characteristic of mononuclear copper(II) complexes with d^9 configuration (S = ½). The frozen solution EPR spectra of the copper(II) complexes showed g_{II} = 2.276 and $g_{\perp}$ = 2.064 for complex **1**, g_{II} = 2.279 and $g_{\perp}$ = 2.062 for complex **3**, g_{II} = 2.261 and $g_{\perp}$ = 2.057 for complex **5** and g_{II} = 2.257 and $g_{\perp}$ = 2.060 for complex **7** indicating the interaction of the unpaired electron with nuclear spin of the copper(II) nucleus (^{63,65}Cu; I = 3/2) [39]. There were no forbidden half filled ($\Delta m = 2$) spectra observed indicating mononuclear nature of the complexes. Similar g_{II} and $g_{\perp}$ values of all the complexes indicate the similar structural behavior of the complexes.

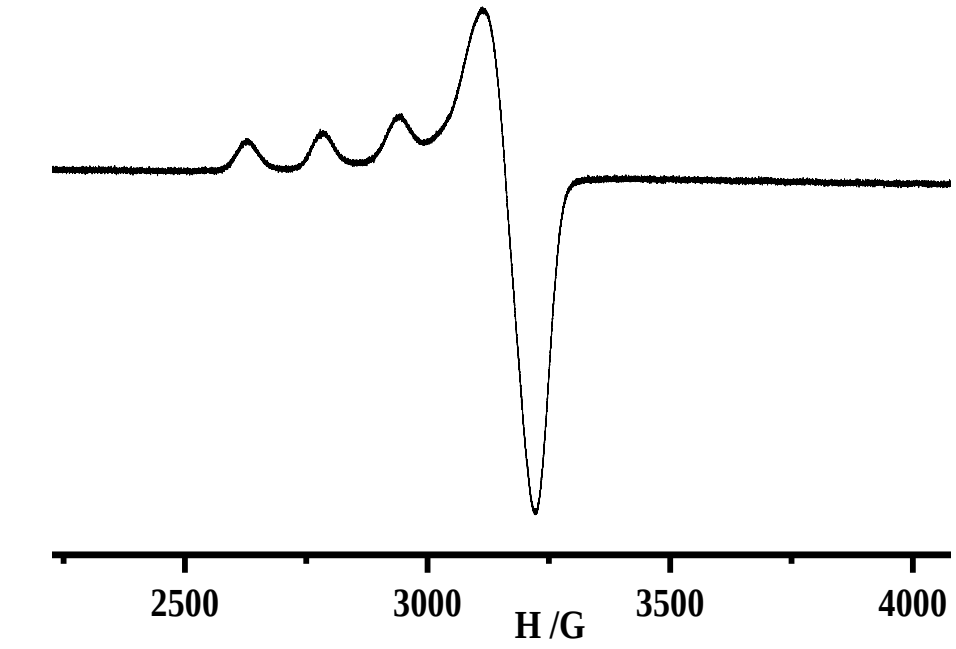

[Cu(bdmpe)Cl]PF_6 (1)

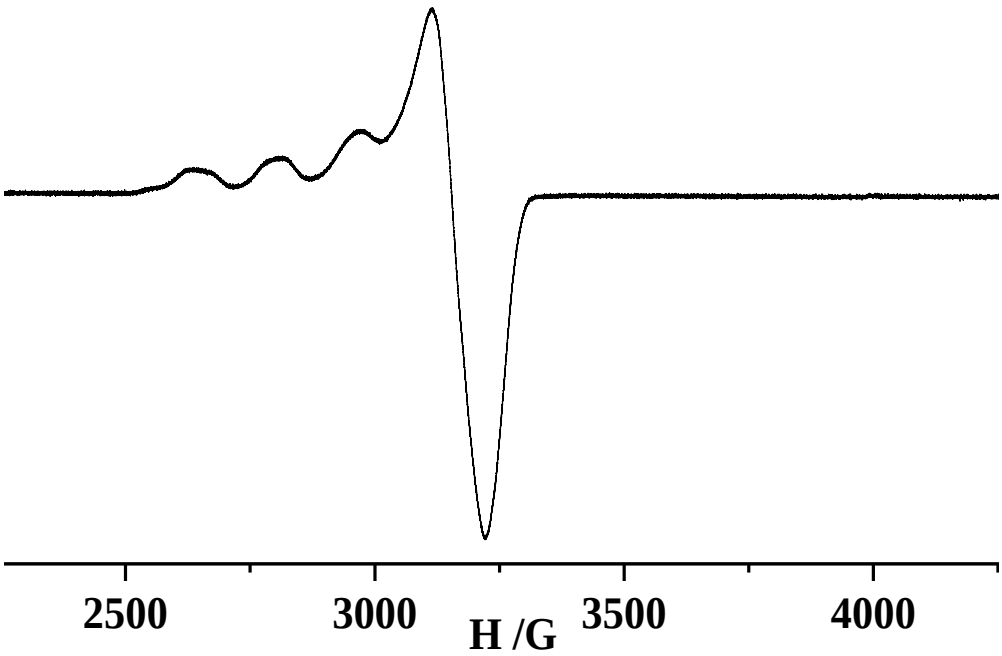

[Cu(bpmpe)Cl]PF_6 (5)

Fig.3(A).14. EPR spectra of complexes **1**and **5** in DMF solution at 77 K.

Room temperature magnetic susceptibility measurements of powder sample of the complexes show that the complexes have magnetic moments close to their spin only value for Cu(II) complexes (S = 1/2) with μ_{eff} ~ 1.75 BM indicating one electron paramgnetism. Mononuclear copper(II) complexes without Cu–Cu interactions shows magnetic moment in the range of 1.75–2.20 BM [40]. Nickel(II) complexes show two electron paramagnetism (S = 1) with μ_{eff} ~ 2.88 BM indicating geometry of the complexes are octahedral.

3(A).4.4. Description of Crystal Structures

3(A).4.4.1. Description of X-ray structures of [Cu(bdmpe)X]PF_6 [X = Cl(1), Br(3)].

The ORTEP diagrams with the atom labeling scheme of the discrete monomeric cations $[Cu(bdmpe)Cl]^+$ of **1** and $[Cu(bdmpe)Br]^+$ of **3** are shown in Fig.3(A).15(a) and 3(A).16. These two monomers have the same basic structure but different bond parameter. A summary of the X-ray crystallographic data and selected bond distance and angles are listed in Table 3(A).1 and 3(A).2. Both complexes are monomeric, isostructural, penta coordinated and crystallized in triclinic crystal system with *P-1* space group. The tetradentate N_3S-ligand bdmpe is coordinated to the copper centre in neutral form via two pyrazolyl nitrogen atoms and one tertiary nitrogen atom and one thiophenyl sulfur atom and forming three five membered chelate rings. In both complexes the copper(II) ion has coordinated with N(1), N(3), N(5) and S(1) from N_3S-ligand bdmpe and the remaining position is occupied by respective Cl(1) or Br(1). A first inspection of the overall coordination geometry around five coordinated copper(II) center can be described as a structure between square-pyramidal (SP) and trigonal–bipyramidal (TBP). The parameter τ has been used to describe the degree of structural distortion from the SP geometry (τ = 0) to the TBP geometry (τ = 1) [41]. The value of Addison parameter τ are 0.23 and 0.06 for complexes **1** and **3**, respectively indicating that the geometry of copper(II) center in both complexes are close to square pyramidal geometry. The basal plane of the geometrical structure of both complexes is formed by two pyrazole nitrogen N(1) and N(5), one tertiary nitrogen N(3) from ligand bdmpe and one respective halide X(1) [X= Cl(1) or Br(1)] and the apical position is occupied by one sulfur atom S(1) from ligand coordinates at a long distance to copper(II) center of both complexes.

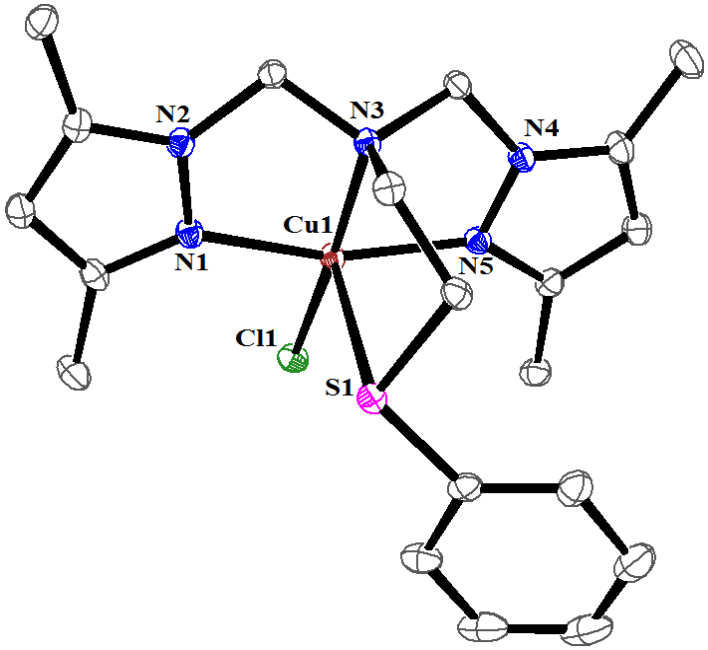

(a)

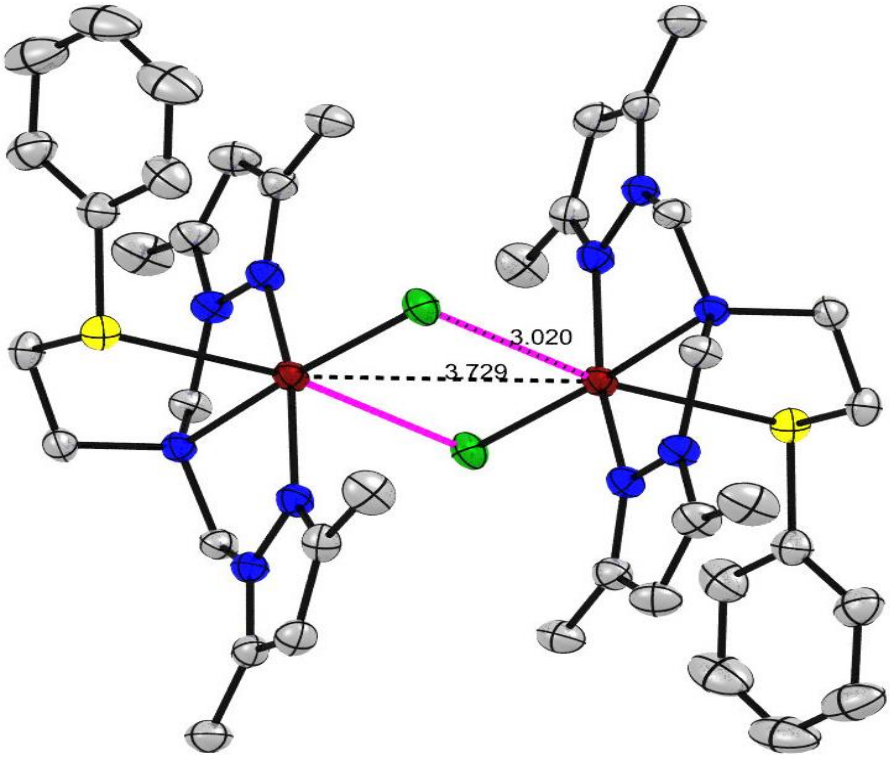

(b)

Fig.3(A).15(a). ORTEP diagram depicting the cationic part of the complex [Cu(bdmpe)Cl]PF_6 (**1**) with atom numbering scheme (40% probability factor for the thermal ellipsoids). **(b).** Perspective view of the supramolecular dimer [{Cu(bdmpe)Cl}]$^{2+}$ of **1**. The non-covalent Cu. . .Cl interactions is shown with magenta dashed lines.

Table 3(A).2. Selected bond lengths (Å) and bond angles (º) for complexes **1**, **3**, **5, 7** and **9.**

Bond lengths (Å)									
[Cu(bdmpe)(Cl)]PF_6 (1)		**[Cu(bdmpe)(Br)]PF_6] (3)**		**[Cu(bpmpe)(Cl)]PF_6 (5)**		**[Cu(bpmpe)(Br)]PF_6 (7)**		**[Ni(bdmpe)(Cl)]$_2$(PF_6)$_2$ .CH_3CN (9)**	
Cu(1)-N(5)	1.9979(16)	Cu(1)-N(5)	1.983(8)	Cu(1)-N(5)	1.952(3)	Cu(1)-N(5)	1.941(3)	Ni(1)-N(5)	2.082(2)
Cu(1)-N(3)	2.1081(15)	Cu(1)-N(1)	1.991(8)	Cu(1)-N(3)	2.129(3)	Cu(1)-N(3)	2.141(3)	Ni(1)-N(3)	2.1316(19)
Cu(1)-N(1)	1.9895(16)	Cu(1)-N(3)	2.110(7)	Cu(1)-N(1)	1.948(3)	Cu(1)-N(1)	1.939(3)	Ni(1)-N(1)	2.069(2)
Cu(1)-S(1)	2.7313(5)	Cu(1)-S(1)	2.668(3)	Cu(1)-S(1)	2.6703(10)	Cu(1)-S(1)	2.6726(10)	Ni(1)-S(1)	2.4353(6)
Cu(1)-Cl(1)	2.2495(5)	Cu(1)-Br(1)	2.3517(16)	Cu(1)-Cl(1)	2.2432(11)	Cu(1)-Br(1)	2.3861(6)	Ni(1)-Cl(1)	2.4533(6)
								Ni(1)-Cl(1i)	2.3629(6)
								Ni(1)-Ni(1i)	3.465

Bond angles (º) for complexes **1**, **3** and **5.**

[Cu(bdmpe)(Cl)]PF_6 (1)		**[Cu(bdmpe)(Br)]PF_6] (3)**		**[Cu(bpmpe)(Cl)]PF_6 (5)**	
Cl(1)-Cu(1)-S(1)	100.625(18)	Br(1)-Cu(1)-S(1)	116.30(7)	Cl(1)-Cu(1)-S(1)	98.06(4)
N(5)-Cu(1)-Cl(1)	99.57(5)	N(5)-Cu(1)-Br(1)	97.9(2)	N(1)-Cu(1)-S(1)	101.51(10)
N(5)-Cu(1)-S(1)	92.39(5)	N(5)-Cu(1)-S(1)	100.3(3)	N(1)-Cu(1)-Cl(1)	97.64(10)
N(5)-Cu(1)-N(3)	81.46(6)	N(1)-Cu(1)-Br(1)	97.7(2)	N(1)-Cu(1)-N(3)	82.06(13)
N(3)-Cu(1)-Cl(1)	175.54(4)	N(1)-Cu(1)-S(1)	80.9(2)	N(1)-Cu(1)-N(5)	161.14(14)
N(3)-Cu(1)-S(1)	83.64(4)	N(1)-Cu(1)-N(5)	161.8(3)	N(3)-Cu(1)-S(1)	83.68(9)
N(1)-Cu(1)-Cl(1)	97.58(5)	N(3)-Cu(1)-Br(1)	158.1(2)	N(3)-Cu(1)-Cl(1)	178.26(9)
N(1)-Cu(1)-S(1)	90.49(5)	N(3)-Cu(1)-S(1)	85.2(2)	N(5)-Cu(1)-S(1)	86.67(10)
N(1)-Cu(1)-N(5)	161.77(7)	N(3)-Cu(1)-N(5)	81.1(3)	N(5)-Cu(1)-Cl(1)	97.99(11)
N(1)-Cu(1)-N(3)	80.98(6)	N(1)-Cu(1)-N(3)	81.0(3)	N(5)-Cu(1)-N(3)	82.00(14)

Bond angles (°) for complexes **7** and **9.**

[Cu(bpmpe)(Br)]PF_6 (7)		**[Ni (bdmpe)(Cl)]$_2$(PF_6)$_2$.CH_3CN (9)**			
Br(1)-Cu(1)-S(1)	96.92(3)	Cl(1)-Ni(1)-S(1)	172.09(2)	Cl(1i)-Ni(1)-N(3)	179.55(6)
N(3)-Cu(1)-Br(1)	179.30(8)	Cl(1i)-Ni(1)-S(1)	93.06(2)	N(3)-Ni(1)-S(1)	86.91(5)
N(3)-Cu(1)-S(1)	83.72(8)	N(5)-Ni(1)-Cl(1)	90.46(6)	N(3)-Ni(1)-N(5)	79.67(8)
N(5)-Cu(1)-Br(1)	98.23(10)	N(5)-Ni(1)-Cl(1i)	100.77(6)	N(1)-Ni(1)-N(3)	80.20(8)
N(5)-Cu(1)-S(1)	87.33(9)	N(5)-Ni(1)-S(1)	81.64(6)	Cl(1)-Ni(1)-Cl(1i)	91.99
N(5)-Cu(1)-N(3)	82.08(12)	Cl(1)-Ni(1)-N(1)	90.12(6)	Ni(1)-Ni(1)-Ni(1i)	88.01
N(1)-Cu(1)-Br(1)	97.66(9)	Cl(1i)-Ni(1)-N(1)	99.36(6)		
N(1)-Cu(1)-S(1)	101.19(9)	N(1)-Ni(1)-S(1)	97.42(6)		
N(1)-Cu(1)-N(3)	81.92(12)	N(1)-Ni(1)-N(5)	159.87(8)		
N(1)-Cu(1)-N(5)	160.91(13)	Cl(1)-Ni(1)-N(3)	92.08(5)		

In complex **1**, the bond distance of equatorial sites Cu-N(1) [1.9895(16)Å], Cu(1)-N(3) [2.1081(15) Å], Cu(1)-N(5) [1.9979(16)Å] and Cu(1)-Cl(1) [2.2495(5)Å] are not equal whereas the long apical site is occupied by sulfur S(1) atom [Cu(1)-S(1) = 2.7313(5)Å]. The Cu(1) center deviates by 0.071Å from its basal N_3Cl plane towards the sulfur atom of ligand bdmpe. Deviation of coordinating atoms N(1), N(3), N(5) and Cl(1) from the mean plane are 0.025, 0.008, 0.025 and 0.014 Å, respectively. In complex **1**, there are three five member chelate rings and their chelate bite angles are N(1)–Cu(1)–N(3) 80.98(6)º, N(3)–Cu(1)–N(5) 81.46(6)º and N(3)–Cu(1)–S(1) 83.64(4)º [42-43]. The shortest Cu….Cu separation is 3.729 Å and the Cu(1). . .Cl(1) [-x, 1-y, 1-z] separation is 3.020 Å, thus formation of supramolecular dimer is observed Fig.3(A).15(b) [44-45].

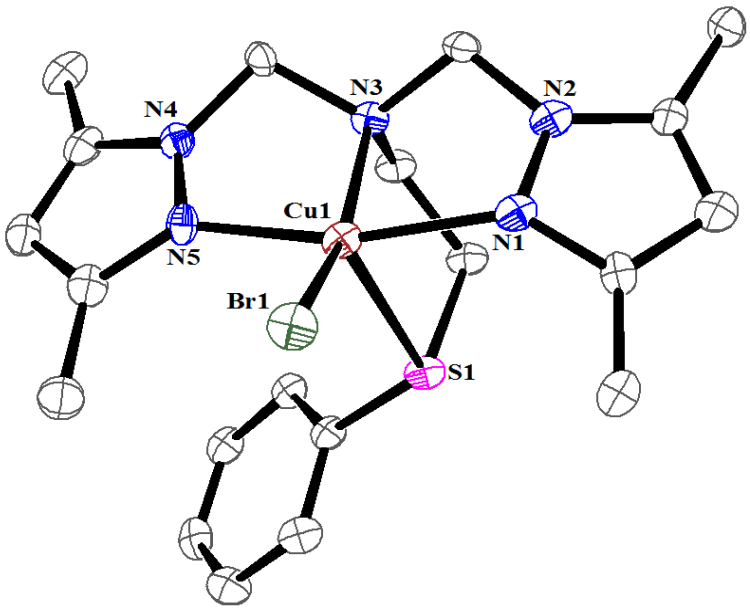

Fig.3(A).16. ORTEP diagram depicting the cationic part of the complex [Cu(bdmpe)(Br)]PF_6 (**3**) with atom numbering scheme (40% probability factor for the thermal ellipsoids).

In complex **3**, the bond distance of equatorial sites are in the range of 1.983(8) – 2.3517(16) Å, whereas the apical site bond distance [Cu(1)-S(1)] is 2.668(3) Å. The Cu(1) center deviates by 0.267 Å from its basal N_3Br plane towards the sulfur atom of ligand bdmpe and Br(1) atom deviates by 0.816 Å from its basal N_3Cu plane. Deviation of coordinating atoms N(1), N(3), N(5) and Br(1) from the mean plane are 0.101, 0.233, 0.101 and 0.182 Å, respectively. There are three five membered chelate rings

with ligand and copper atom and their chelate bite angles are N(1)–Cu(1)–N(3) 81.0(3), N(3)–Cu(1)–N(5) 81.1(3)and N(3)–Cu(1)–S(1) 85.2(2) [42-43].

3(A).4.4.2. Description of X-ray structures of [Cu(bpmpe)X]PF_6 [X = Cl(5), Br(7)].

The ORTEP diagrams with the atom labeling scheme of the discrete monomeric cations $[Cu(bpmpe)Cl]^+$ of **5** and $[Cu(bpmpe)Br]^+$ of **7** are shown in Fig.3(A).17 and 3(A).18(a). The two monomers have same basic structure but different bond parameters. Both complexes **5** and **7** are isostructural, five coordinated and crystallized in monoclinic crystal system with *$P2_1/n$* space group. For both synthesized compounds tetra dentate N_3S-ligand bpmpe acts as a chelate ligand and its coordination to the copper ion in neutral form via two pyrazolyl nitrogen atoms and one tertiary nitrogen atom and one thiophenyl sulfur atom, thus forming three fused five membered chelate rings. In both complexes the copper(II) ion has five coordination with N(1), N(3), N(5) and S(1) from N_3S-ligand bdmpe and the remaining position is occupied by Cl(1) or Br(1). The structural distortion indexes are 0.29 and 0.31 for complexes **5** and **7**, respectively indicating that Cu(II) polyhedron are close to square pyramidal (4+1 (SP)) geometry for both complexes. The basal plane of the said geometrical structure is formed by two pyrazole nitrogen N(1) and N(5), one tertiary nitrogen N(3) from ligand bpmpe and one respective halide X(1) [X= Cl(1) or Br(1)] and the apical position is occupied by one sulfur atom S(1) from ligand bpmpe with a long distance to copper(II) center in both complexes.

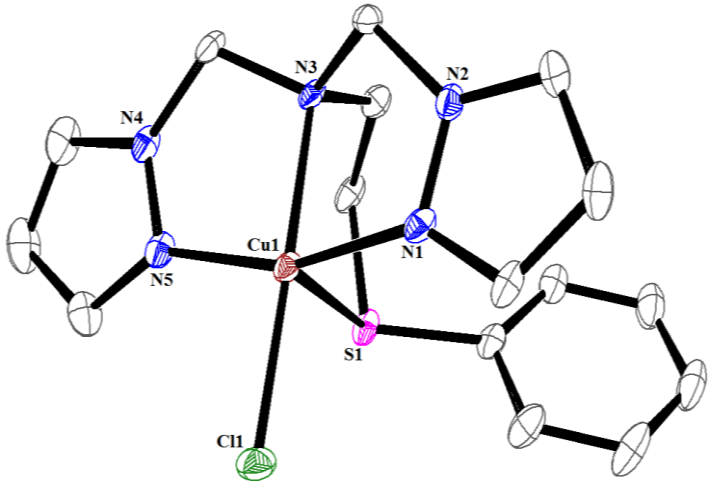

Fig.3(A).17. ORTEP diagram depicting the cationic part of the complex [Cu(bpmpe) Cl]PF_6 (**5**) with atom numbering scheme (40% probability factor for the thermal ellipsoids).

The bond distance of two equatorial sites of Cu-N(1) [1.948(3) Å] and Cu(1)-N(5) [1.952(3) Å] are different from the other two Cu(1)-N(3) [2.129(3) Å] and Cu(1)-Cl(1) [2.2432(11)Å] distances whereas the apical bond distance [Cu(1)-S(1)] is 2.6703(10) Å. The Cu(1) center deviates by 0.103Å from its basal N_3Cl plane towards the sulfur atom of ligand bpmpe. Deviations of coordinating atoms N(1), N(3), N(5) and Cl(1) from the mean plane are 0.090, 0.061, 0.090 and 0.037 Å, respectively. The tripodal ligand form are three five membered chelate rings and their chelate bite angles are N(1)–Cu(1)–N(3) 82.06(13), N(3)–Cu(1)–N(5) 82.00(14)and N(3)–Cu(1)–S(1) 83.68(9) [42-43].

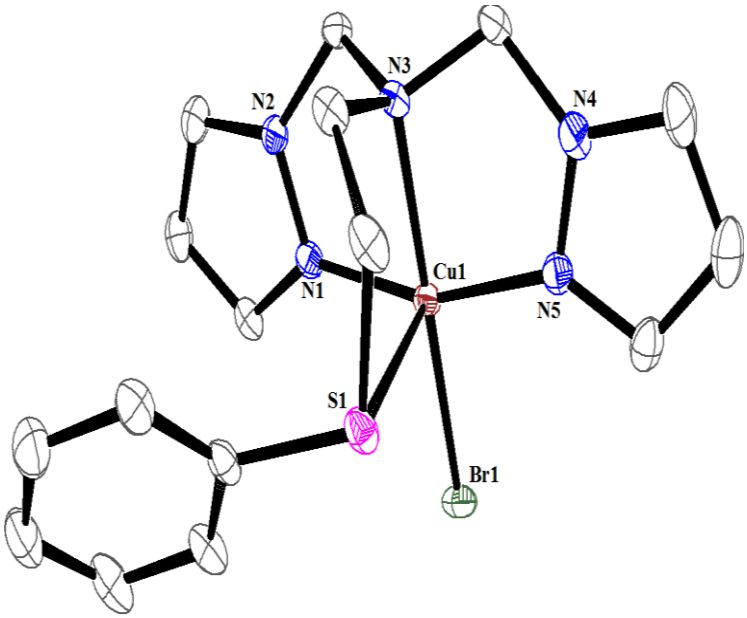

Fig.3(A).18(a). ORTEP diagram depicting the cationic part of the complex [Cu(bpmpe)Br]PF_6 (**7**) with atom numbering scheme (40% probability factor for the thermal ellipsoids).

In complex **7**, the bond distance of equatorial sites are in the range of 1.939(3) - 2.3861(6)Å, whereas the apical site bond distance [Cu(1)-S(1)] is 2.6726(10)Å. The Cu(1) center deviates by 0.094 Å from its basal N_3Br plane towards the sulfur atom of ligand bpmpe. Deviation of coordinating atoms N(1), N(3), N(5) and Br(1) from the mean plane are 0.1, 0.078, 0.099 and 0.047 Å, respectively. In the complex there are three five membered chelate rings and their chelate bite angles are N(1)–Cu(1)–N(3) 81.92(12), N(3)–Cu(1)–N(5) 82.08(12)and N(3)–Cu(1)–S(1) 83.72(8) [42-43].The shortest Cu. . .Cu and Cu(1). . .Br(1) [2-x, 1-y, 2-z] separation are 3.878 and 3.248 Å respectively, thus formation of supramolecular dimer is observed [Fig. 3(A).18(b)] [44-45].

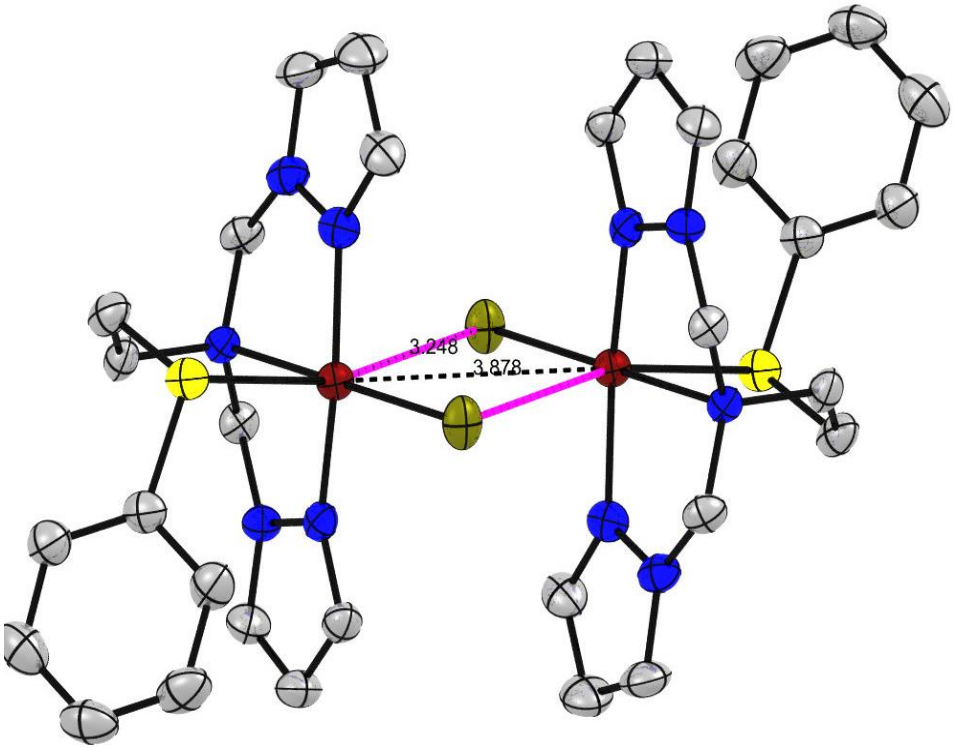

Fig.3(A).18(b). Perspective view of the supramolecular dimer $[\{Cu(bpmpe)Br\}]^{2+}$ of **7**. The non-covalent Cu. . .Br interactions are shown with magenta dashed lines.

3(A).4.4.3. Description of X-ray structure of $[Ni(bdmpe)\mu\text{-}Cl]_2(PF_6)_2.CH_3CN$ (9).

Single crystal structure determination data reveals that above titled compound crystals are made up of dimeric $[Ni(bdmpe)(\mu\text{-}Cl)]_2^{2+}$ cations isolated by two PF_6 counter anion and crystallize in triclinic crystal system with *P-1* space group. The ORTEP diagram with the atom labelling scheme of complex clearly shows that it is a centrosymmetric, dichloride-bridged binuclear nickel(II) complex with a $[Ni_2(\mu\text{-}Cl)_2]$ core unit [Fig. 3(A).19.]. Table 3(A).1 summaries crystal data, intensity data, collection details and refinement parameters and Table 3(A).2 lists the selected bond distances and angles involving metal atom. In the dimeric cation, the two six-coordinate nickel(II) centers are bridged by two chloride ion and each nickel center is bonded to a tetradentate N_3S-ligand bdmpe. So the geometry of nickel atom can be described as a distorted octahedral.

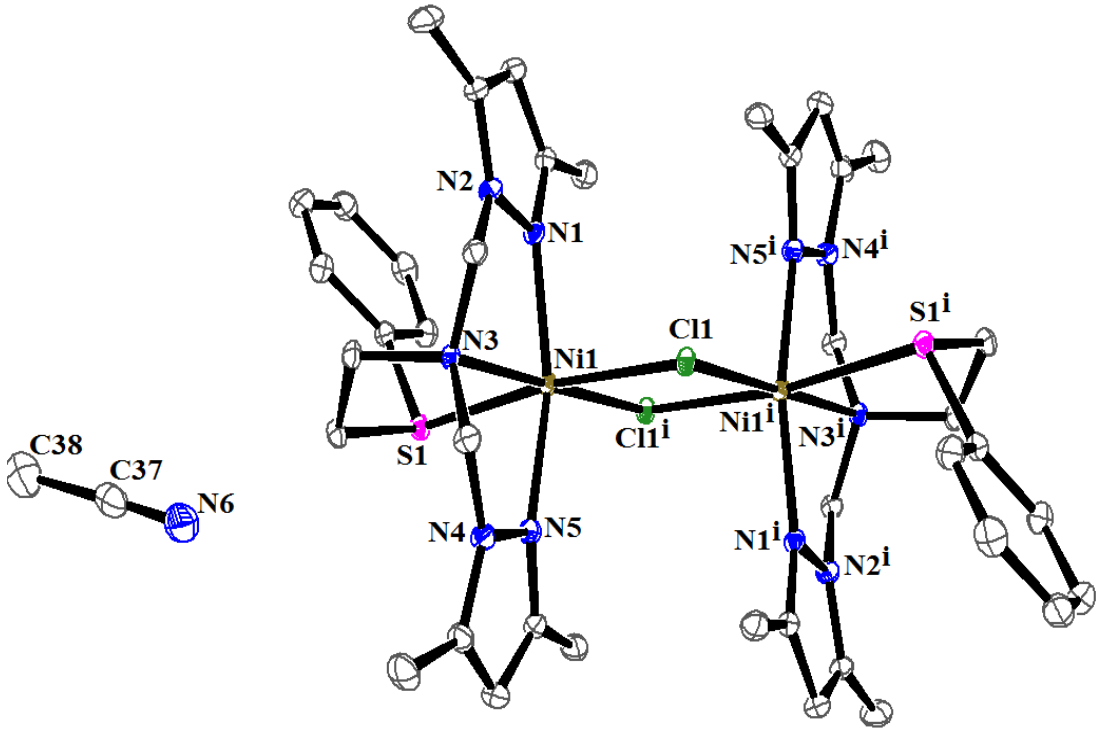

Fig.3(A).19. ORTEP diagram depicting the cationic part of the complex [Ni(bdmpe)μ-Cl]$_2$(PF$_6$)$_2$.CH$_3$CN (**9**) with atom numbering scheme (40% probability factor for the thermal ellipsoids).

In the equatorial plane, each nickel(II) ions are coordinated by two nitrogens N(1) and N(5) of pyrazole rings and one tertiary nitrogen N(3) of ligand bdmpe and one of chloride atom Cl(1) from chloride bridge and axial position occupied by remaining chloride bridge chlorine atom Cl(1i) and one sulfur atom S(1) from ligand bdmpe. Three equatorial bonds are nearly equal Ni(1)-N(1) [2.069(2) Å], Ni(1)-N(3) [2.1316(19) Å], Ni(1)-N(5) [2.082(2) Å] but shorter than Ni(1)-Cl(1i) [2.3629(6) Å] and two axial bonds Ni(1)-S(1) [2.4353(6) Å] and Ni(1)-Cl(1) [2.4533(6) Å] are nearly equal. Ligand bdmpe form three five membered chelate rings in each nickel centers and their bite angles are N(1)-Ni(1)-N(3) [80.20(8)º], S(1)-Ni(1)-N(3) [86.91(5)º] and N(5)-Ni(1)-N(3) [79.67(8)º] [46-47]. The bridging Ni_2Cl_2 unit is strictly planar due to the presence of crystallographic inversion center in the middle of the dimer and four pyrazoles and two phenyl rings are in anti-position with respect to Ni_2Cl_2 core. The intra-dimer Ni(1). . .Ni(1i) distance is 3.465 Å and Cl(1)-Ni(1)-Cl(1i) bond angle is 88.01(2)º. The nickel-nickel distance is good agreement with reported double chloride bridged binuclear Ni(II) complexes [48]. The chlorine double bridge within the dimer is asymmetric because the Ni-Cl bond lengths are 2.3629(6) Å and 2.4533(6) Å and a

bridging angle Ni(1)-Cl(1)-Ni(1i) 91.99(2)º. The unequal bond lengths produce distortion in the molecule.

3(A).4.5. Cleavage experiment

To find out effective synthetic compounds with DNA cleavage activity, the interaction of plasmid pBS KS(+) with the compounds in the presence of H_2O_2 was studied. The results of plasmid DNA cleavage by the complexes are shown in Fig. 3(A).20. In all the tests, thick bands were observed in the controls viz. untreated plasmid, plasmid with H_2O_2 only and plasmid with complexes (50 µM) only in lane 1, lane 2 and lane 3 respectively. This suggested that the plasmid was intact without treatment and with H_2O_2 and the complexes alone had no effect on the plasmid. In case of complex **1**, **3** and **7** the absence of the DNA bands even in the lane 4, very clearly revealed that the complexes effectively cleaved the DNA at the low concentration of 10 µM. The cleavage effect was prominent in lane **4** with decrease in band intensity. In case of complex **5**, the complete disappearance of bands was observed from lane 5 onwards suggesting 50 µM and higher will be the effective concentrations. The complex **9** apparently had no significant DNA cleavage effect, as no difference in the bands intensity of control and treated lanes on the gel was seen. The transition metal like copper reacts with dioxygen in the presence of a reductant often generate reactive oxygen species that eventually may cleave DNA [8, 49]. The cleavage is thought to occur by oxidative mechanism and initiated by the generation of reactive oxygen species such as the hydroxyl radical or singlet oxygen through a Fenton type mechanism. All the compounds were suspected to cleave in a catalytic manner as shown by complete disappearance of bands after treatment with the complex and absence of any form of the plasmid DNA (supercoiled, linear, nicked circular). On the basis of the results it is evident that the complexes **1**, **3**, **5** and **7** are effective DNA cleavage agents. The results highlight the cumulative effect of the constituents in complexes and emphasizes on selecting certain combinations over other. The metal complexes are centre of attraction in the efforts to find out artificial nucleases [50-51] to replace the costly and difficult to commercially produce natural agents and the compounds studied above can lay a way to this.

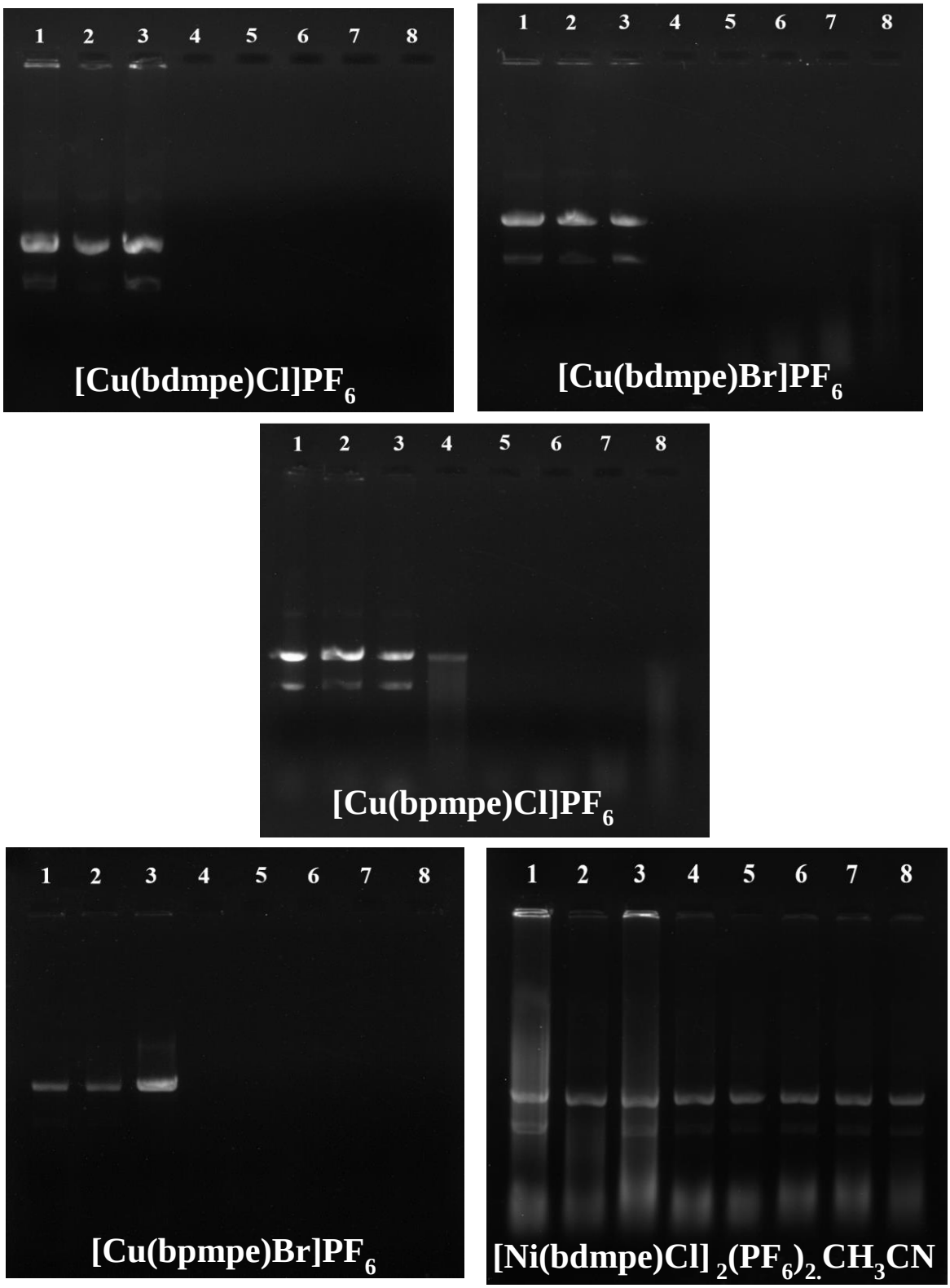

Fig.3(A).20. Cleavage of DNA(pbs KS(+)) induced by complexes: Lane 1, untreated DNA; lane 2, plasmid DNA + 3 µl H_2O_2; lane 3, plasmid DNA + 50 µM complex; lane 4, plasmid DNA + 10 µM complex + 3 µl H_2O_2; lane 5, plasmid DNA + 20 µM complex + 3 µl H_2O_2; lane 6, plasmid DNA + 30 µM complex + 3 µl H_2O_2; lane 7, plasmid DNA + 40 µM complex + 3 µl H_2O_2; lane 8, plasmid DNA + 50 µM complex + 3 µl H_2O_2, respectively.

3(A).4.6. Antimicrobial activity

The Cu(II) complexes with the resolved structure were studied for their antimicrobial activity against *Bacillus subtilus*, *Streptococcus aureus*, *Escherichia Coli* and *Pseudomonas aeruginosa* as shown in Table. 3(A).3. Absence of inhibition the negative control plate and strong inhibition in the presence of chloramphenicol proved the susceptibility of microorganisms to antimicrobial agents.

Table 3(A).3. Antimicrobial activity data of the salts, ligands and complexes **1**, **3**, **5, 7, 9**.

Compound	**MIC value in mM**			
	S. aureus	***B. Subtilis***	***E. coli***	***P. aeruginosa***
$CuCl_2.2H_2O$	>10	>10	10	>10
$CuBr_2.4H_2O$	>10	>10	>10	>10
$NiCl_2.6H_2O$	>10	>10	>10	>10
bdmpe	>10	10	>10	>10
bpmpe	>10	10	>10	10
[Cu(bdmpe)Cl]PF_6 (1)	10	5	>10	>10
[Cu(bdmpe)Br]PF_6 (3)	10	5	5	10
[Cu(bpmpe)Cl]PF_6 (5)	10	10	>10	10
[Cu(bpmpe)Br]PF_6 (7)	10	>10	>10	>10
[Ni(bdmpe)Cl]$_2$(PF_6)$_2$.(CH_3CN) (9)	>10	10	10	10

Complex [Cu(bdmpe)Br]PF_6 **3** was found to be effective against all the four tested micro-organisms with more activity against *Bacillus sublitus* (Gram positive) and *Escherichia coli* (Gram negative) with an MIC of 5 µM then against *Streptococcus aureus* (Gram positive) and *Pseudomonas aeruginosa* (Gram Negative) with an MIC of 10 µM. This suggested that the mode of action was independent of cell wall composition. Complex [Cu(bdmpe)Cl]PF_6 **1** displayed activity against both Gram positive bacteria with an MIC of 10 µM against *Streptococcus aureus* and 5 µM against

Bacillus subtilus. Complex **3** effectively inhibited the growth of all the organisms with MIC of 10 µM against *Streptococcus aureus* and *Pseudomonas aeruginosa* and 5 µM against *Escherichia coli* and *Bacillus subtilus*. Complex **5** was active against all except *E.coli* with MIC of 10 µM and Complex **7** was active against *Streptococcus aureus* only with an MIC of 10 µM. The complex 9 could inhibit all but *Streptococcus aureus* with an MIC of 10 µM. The complex **3** considerably inhibited *Bacillus subtilus* and *Escherichia coli* and displayed activity against all the microorganisms. The MIC of bdmpe derived copper(II) complexes in all the cases, was either equal to or less than those derived from bpmpe, suggesting good antimicrobial activity of copper complexes derived from bdmpe over bpmpe. The complex **9** inhibited the gram negative micro-organisms (*Escherichia coli* and *Pseudomonas aeruginosa*) better than ligand bdmpe and metal salt, as was suggested by the decrease in MIC. Overall the complexes showed better antimicrobial activity then the constituent groups and ligands as shown by the decrease in MIC in case of complexes [52], except in case of *Escherichia coli* where $CuCl_2.2H_2O$ was more effective than the corresponding complexes **1** and **5**. The improvement in activity can be attributed to the presence of metal ions which influence the solubility, conductivity and dipole moment of the complexes which could be the significant factors responsible for increasing the penetration of the molecules into bacterial cell wall, effectively targeting the bacterial machinery by various mechanisms [53].

3(A).5. Conclusion

Binuclear nickel(II) complexes $[Ni(bdmpe)(\mu\text{-}Cl)]_2(Y)_2.CH_3CN$ and mononuclear five coordinated copper(II) halides complexes of the type [Cu(bdmpe/bpmpe)X]Y [X = Cl/ Br and Y = PF_6^-/ BF_4^-] have been synthesized by the reaction of respective metal halides with ligands *N*,*N*-bis((3,5-dimethyl-1H-pyrazol-1-yl)methyl)-2-(phenylthio)ethan-1-amine (bdmpe) or *N*,*N*-bis((1H-pyrazol-1-yl)methyl)-2-(phenylthio)ethan-1-amine (bpmpe) in the presence of PF_6^- or BF_4^- and characterized. Structural data show all copper complexes are mononuclear with square pyramidal geometry whereas binuclear nickel(II) complex has distorted octahedral geometry where two chloride ions bridged between the two nickel centers. The antimicrobial activities of the above complexes showed moderate activity against Gram positive and Gram negative bacteria. Complex $[Cu(bdmpe)Br]PF_6$ showed maximum inhibition against all the test microorganisms and complexes $[Cu(bpmpe)Cl]PF_6$ and $[Ni(bdmpe)Cl]_2(PF_6)_2$ showed activity against all except *Escherichia coli* and *Streptococcus aureus* respectively. The characteristic of the complexes can lead to novel, effective and economical DNA cleavage agents. $[Cu(bdmpe/bpmpe)X]PF_6$ complexes proved to be effective cleavage agents as was evident from their activity even at very low concentrations whereas no significant effect on DNA cleavage was seen in case of Ni(II) complex.

3(A).6. References:

1. P.J. O'Dwyer, J.P. Stevenson, S.W. Johnson, in: B. Lippert (Ed.), Chemistry and Biochemistry of Leading Anticancer Drug: Clinical Status of Cisplatin, Carboplatin and Other Platinum-based Antitumor Drugs, Wiley-VCH, Zurich, 1999.
2. T.K. Goswami, B.V.S.K. Chakravarthi, M. Roy, A.A. Karande, A.R. Chakravarty, Inorg. Chem. 50 (2011) 8452.
3. M.F. Primik, G. Muhlgassner, M.A. Jakupec, O. Zava, P.J. Dyson, V.B. Arion, K. Bernhard, B.K. Keppler, Inorg. Chem. 49 (2010) 302.
4. M. Pait, B. Kundu, S.C. Kundu, D. Ray, Inorg. Chim. Acta 418 (2014) 30.
5. F. Silva, C. Fernandes, M.P.C. Campello, A. Paulo, Polyhedron 125 (2017) 186.
6. J.Y. Minenkov, A. Singstad , G. Occhipinti, V.R. Jensen, Dalton Trans. 41 (2012) 5526..
7. W. Liua, R. Gust, Chem. Soc. Rev. 42 (2013) 755.
8. P.U. Maheswari, K. Lappalainen, M. Sfregola, S. Barends, P. Gamez, U. Turpeinen, J. Reedijk, Dalton Trans. 33 (2007) 3676.
9. I. Romero-Canelon, P. J. Sadler, Inorg. Chem. 52 (2013) 12276.
10. Y. Jin, J.A. Cowan, J. Am. Chem. Soc. 127(2005) 8408.
11. K. Zheng, L. Jiang, Y.-T. Li, Z.-Y. Wu, C.-W. Yan, RSC Adv. 5 (2015) 51730.
12. S. Mukherjee, C. Basu, S. Chowdhury, A.P. Chattopadhyay, A. Ghorai, U. Ghosh, H. Stoeckli-Evans, Inorg. Chim. Acta 363 (2010) 2752.
13. N. Deibel, M.G. Sommer, S. Hohloch, J. Schwann, D. Schweinfurth, F. Ehret, B. Sarkar, Organometallics 33 (2014) 4756.
14. K.K.-W. Lo, S.P.-Y. Li, RSC. Adv. 4 (2014) 10560.
15. R.H. Ismayilov, W.Z. Wang, G.H. Lee, C.Y. Yeh, S.A. Hua, Y. Song, M.M. Rohmer, M. Bénard, S.M. Peng, Angew. Chem. Int. Ed. 50 (2011) 2045.
16. R.N. Mukharjee, Coord. Chem. Rev. 203 (2000) 151.
17. Y. Zhou, W. Chen, Organometallics 26 (2007) 2742.
18. Y. Han, H.V. Huynh, Chem. Commun. (2007) 1089.
19. J.M. Gonzalez-Perez, D. Choquesillo-Lazarte, A. Dominguez-Martin, E. Vílchez-Rodriguez, I. Perez-Toro, A. Castineiras, O.K. Arriortua, M.E. Garcia-Rubino, A. Matilla-Hernandez, J. Niclos-Gutierrez, Inorg. Chim. Acta

452 (2016) 258.

20. M. Kalita, P. Gogoi, P. Barman, B. Sarma, A.K. Buragohain, R.D. Kalita, Polyhedron 74 (2014) 93.
21. X.Z. Zou, J.A. Zhang, L.J. Zhang, Y.J. Liu, N. Li, Y. Li, S.C. Wei, M. Pan, Inorg. Chem. Commun. 54 (2015) 21.
22. S.B. Kumar, M. Zala, A. Solanki, R. Mohammedayaz, P. Parikh, E. Suresh, Polyhedron 36 (2012) 15.
23. M.H. Sadhu, A. Solanki, S.B. Kumar, Polyhedron 100 (2015) 206.
24. H.C. Bimboim, J. Doly, Nucl. Acids Res. 7(6) (1979) 1513.
25. J. Marmur, J. Mol. Biol. 3 (1961) 208.
26. M.E. Reichmann, S.A. Rice, C.A. Thomas, P. Doty, J. Am. Chem. Soc. 76 (1954) 3047.
27. A.R. Katritzky, X. Yong-Jiang, H. Hai-Ying, S. Mehta, J. Org. Chem. 66 (2001) 5590.
28. Agilent, CrysAlis PRO. Agilent Technologies UK Ltd, Yarnton, England, (2011).
29. G.M. Sheldrick, SAINT, 5.1 ed. Siemens Industrial Automation Inc., Madison, WI, (1995)
30. G.M. Sheldrick. SHELXL-97: Program for Crystal Structure Refinement, University of Gottingen, Gottingen, (1997).
31. L.J. Farrugia, J. Appl. Cryst. 32 (1999) 837.
32. L.J. Farrugia, J. Appl. Cryst. 30 (1997) 565.
33. W.J. Geary, Coord. Chem. Rev.7 (1971) 81.
34. K. Nakamoto, Infrared and Raman Spectra of Inorganic and Coordination Compounds, 3rd edn. Wiley Interscience, New York, (1978).
35. B.J. Hathaway, in: G. Wilkinson, R.D. Gillard, J.A. McCleverty (Eds.), Comprehensive Coordination Chemistry, vol. 5, Pergamon Press, Oxford, England, (1987) 533.
36. F.A. Moutner, C.N. Landry, A.A. Gallo, S.S. Massoud, J. Mol. Struct. 837 (2007) 72.
37. F.A. Moutner, C.N. Landry, A.A. Gallo, S.S. Massoud, J. Mol. Struct. 837 (2007) 72.
38. U. Mukhopadhayay, I. Bernal, S.S. Massoud, F.A. Moutner, Inorg. Chim.

Acta 357 (2004) 3673.

39. N. Singh, J. Niklas, O. Poluektov, K.M. Van Heuvelen, A. Mukherjee, Inorg. Chim. Acta 455 (2017) 221.
40. N. Wei, N.N. Murthy, K.D. Karlin, Inorg. Chem. 33 (1994) 6093.
41. A.W. Addison, T.N. Rao, J.Reedijk, J.V. Rijn, G.C. Verschoor, J. Chem. Soc. Dalton Trans. (1984) 1349.
42. Y. Funasako, M. Nosho, T. Mochida, Dalton Trans. 42 (2013) 10138.
43. T.E. Patten, M.M. Olmstead, C. Troeltzsch, Inorg. Chim. Acta 361 (2008) 365.

44 R. Herchel, Z. Dvorak, Z. Travnicek, M. Mikuriya, F.R. Louka, F.A. Mautner, S.S. Massoud, Inorg. Chim. Acta 451 (2016) 102.

45. M.H. Sadhu, S.B. Kumar, J.K. Saini, S.S. Purani, T.R. Khanna, Inorg. Chim. Acta 466 (2017) 219.
46. Y. Shimazaki, S. Huth, S. Karasawa, S. Hirota, Y. Naruta, O. Yamauchi, Inorg. Chem. 43 (2004) 7816.
47. W.-Z. Lee, H.-S. Tseng, T.-S. Kuo, Dalton Trans. (2007) 2563.
48. W.-Z. Lee, T.-L. Wang, H.-S. Tsang, C.-Y. Liu, C.-T. Chen, T.-, S. Kuo, Organometallics 28 (2009) 652.
49. T.D. Tullius, J.A. Greenbaum, Curr. Opin. Chem. Biol. 9 (2005) 127.
50. M.J. Fernandez, B.Wilson, M. Palacios, M.M. Rodrigo, K.B. Grant, A. Lorente, Bioconjugate Chem. 18(1) (2007) 121.
51. Y. Jin, J.A. Cowan, J. Am. Chem. Soc. 127(23) (2005) 8408.
52. I.P. Ejidike, P.A. Ajibade, Molecules 20(6) (2015), 9788.

53 Z.H. Chohan, H. Pervez, A. Rauf, A. Scozzafava, C.T. Supuran, J. Enzyme Inhib. Med. Chem. 17(2) (2002) 117.

Abstract

Four mononuclear copper(II) complexes [Cu(bdmpe)X]Y, one mononuclear cobalt(II) complex [Co(bdmpe)$(NCS)_2$] and two binuclear cobalt(II) complexes [Co(bdmpe)$(N_3)]_2Y_2$, where X = NCS^-, NO_2, Y = PF_6^- / ClO_4^- have been synthesized using N_3S-coordinating ligand *N*,*N*-bis((3,5-dimethyl-1*H*-pyrazol-1-yl)methyl)-2-(phenylthio)ethan-1-amine(bdmpe) and characterized by microanalyses, IR, UV-Vis spectra, magnetic study and EPR data. Single crystal X-ray structural data confirmed that the copper(II) complexes [Cu(bdmpe)X]ClO_4 [X = NCS, NO_2] are five coordinated with distorted square pyramidal geometry, complex [Co(bdmpe)$(NCS)_2$] is five coordinated with distorted trigonal bipyramidal geometry and binuclear cobalt(II) complex [Co(bdmpe)$(N_3)]_2(ClO_4)_2$ has distorted octahedral geometry where the two cobalt centre is bridged by two azide ions with end-on coordination mode.

3(B).1. Introduction

Pseudohalides like NCS^-, NCO^-, N_3^- etc are called ambidentate ligand and can coordinate with metal ions with different coordination modes [1-6]. When they bind with metal ions as monodentate ligand, they form mononuclear complexes [7-12] and while acting as bridging ligand, they use different coordination modes- end-to-end (μ-1,3) or end-on (μ-1,1) and form di- or polynuclear complexes using different blocking ligand [13-18]. Pyrazolyl containing tripodal ligands are very interesting chelating ligand and having coordination properties suitable for giving stable metal complexes [19-22]. Transition metal complexes with tripodal pyrazolyl based ligands have rich coordination chemistry. Recently we have synthesized and structurally characterized copper(II), cobalt(II), nickel(II), zinc(II) and cadmium(II) complexes with N_4-coordinate tetradentate ligand and studied their bridging and magnetic properties. It is reported that sulphur coordinating multidentate ligand has bioactivity and has important applications. As our interest is in the synthesis and structurally characterization of pseudohalides containing transition metal complexes with new pyrazolyl containing chelate ligand, we are interested to study the coordination behavior of copper(II) and cobalt(II)complexes with new tetradentate N_3S coordinate ligand *N*,*N*-bis((3,5-dimethyl-1H-pyrazol-1-yl)methyl)-2-(phenylthio)ethan-1-amine (bdmpe) in presence of co-ligand N_3^-, NCS^- and NO_2^-.

In this chapter, we report on the synthesis and characterization of NCS^- / N_3^- / NO_2^- containing copper(II) and cobalt(II) complexes with *N*,*N*-bis((3,5-dimethyl-1H-pyrazol-1-yl)methyl)-2-(phenylthio)ethan-1-amine (bdmpe). Crystal structures of two copper complexes $[Cu(bdmpe)(X)]ClO_4$ [X = NCS, NO_2] and two cobalt(II) complexes $[Co(bdmpe)(NCS)_2]$ and $[Co(bdmpe)(\mu_{1,1}\text{-}N_3)]_2(ClO_4)_2$ have been discussed in detail.

3(B).2. Experimental

3(B).2.1. Materials

The chemicals and solvents were analytical grade and purchased from commercial sources. Acetylacetone, paraformaldehyde, hydrazine hydrate, NaN_3, KNCS, KNCO, $NaNO_2$, copper(II) nitrate hexahydrate (Loba, India), cobalt(II) nitrate hexahydrate, benzenethiol, 2-chloroethan-1- amine hydrochloride, NH_4BF_4, NH_4PF_6 (Aldrich) were reagent grade and used as received. 2-(arylsulfanyl)ethan-1-amine [23], *N*-(3,5-dimethyl-1H-pyrazole-1-yl)methanol [24] and *N*,*N*-bis((3,5-dimethyl-1H-pyrazol-1-yl)methyl)-2-(phenylthio)ethan-1-amine (bdmpe) [25] were synthesized as per the reported procedures. Copper(II) perchlorate hexahydrate and cobalt(II) perchlorate hexahydrate were prepared by reaction of copper carbonate and cobalt carbonate respectively with dilute $HClO_4$ acid and followed by slow evaporation on steam bath.

3(B).2.2. Syntheses of Complexes

Caution! Transition metal complexes with perchlorate ion and organic ligands are potentially explosive. Only a small amount of material should be synthesized and it should be handled with care.

3(B).2.2.1. Synthesis of [Cu(bdmpe)(NCS)]ClO_4 (1)

A mixture of $Cu(ClO_4)_2.6H_2O$ (0.185 g, 0.5 mmol) and ligand bdmpe (0.186 g, 0.5 mmol) were stirred in methanol (25 mL) at room temperature. A methanol solution of KNCS (0.050 g, 0.5 mmol) was added slowly and stirring was continued for 3h at room temperature. Then the resulting solution was filtered and filtrate was allowed to stand in the refrigerator for slow evaporation. Dark green color single crystals suitable for X-ray diffraction were obtained after one week. The crystals were collected by filtration and dried in air.

Yield. 0.108 g (73%). Found C = 42.54, H = 4.79, N = 14.40%. Anal calc for $C_{21}H_{27}ClCuN_6O_4S_2$: C = 42.71, H = 4.61, N = 14.23%. IR (KBr pellet) cm^{-1}: ν(NCS^-), 2094; ν(C = C), 1578 s; ν(C = C) + ν (C = N)/pz ring, 1553 s, 1448 s; ν(C-S), 648 w; ν(ClO_4^-), 1087 br; δ(O–Cl–O), 623 s. UV-Vis spectra: λ_{max}/nm (ε_{max}/$mol^{-1}cm^{-1}$). 663 (174), 285 (2960), 249 (10330), 225 (19585). Λ_M ($\Omega^{-1}cm^2\,mol^{-1}$) = 121. μ_{eff} = 1.76 BM.

3(B).2.2.2. Synthesis of [Cu(bdmpe)(NCS)]PF_6 (2)

A solution of ligand bdmpe (0.186 g, 0.5 mmol) in methanol (10 ml) was added to a solution of $Cu(NO_3)_2.6H_2O$ (0.176 g, 0.5 mmol)in methanol (10 ml) with stirring and the reaction mixture was allowed to stir at room temperature for 10 min. A solution of KNCS (0.050 g, 0.5 mmol) (in 2 drops of water + 5 ml methanol) was added into it. The resulting dark green color solution was mixed with NH_4PF_6 (0.084 g, 0.5 mmol) in methanol (10 ml). The reaction mixture was further stirred for 3h at room temperature. Then the resultant solution was filtered and filtrate was allowed to stand in the refrigerator for slow evaporation. Dark green color single crystals suitable for X-ray diffraction were obtained after one week. The crystals were collected by filtration and dried in air.

Yield. 0.118 g (74%). Found C = 39.81, H = 4.33, N = 13.43%, Anal calc for $C_{21}H_{27}PCuN_6F_6S_2$: C = 39.65, H = 4.28, N = 13.21%. IR (KBr pellet) cm^{-1}: ν(NCS^-), 2048 vs ; ν(C = C), 1584 s; ν(C = C) + ν (C = N)/pz ring, 1555 s, 1466 s; ν(C-S), 656 w; ν(PF_6^-), 839 s. UV-Vis spectra: λ_{max}/nm (ε_{max}/$mol^{-1}cm^{-1}$). 663 (190), 286 (2868), 248 (10349), 224 (20029). Λ_M ($\Omega^{-1}cm^2\,mol^{-1}$) = 118. μ_{eff} = 1.72 BM.

3(B).2.2.3. Synthesis of [Cu(bdmpe)(NO_2)]ClO_4 (3)

This complex was prepared by following the same procedure as that of complex **1**, however, KNCS has been substituted with $NaNO_2$.

Yield. 0.113 g (78%). Found C = 41.75, H = 4.57, N = 14.76%. Anal calc for $C_{20}H_{27}ClCuN_6O_6S$: C = 41.52, H = 4.70, N = 14.53%. IR (KBr pellet) cm^{-1}: ν_{asym}(N-O),1381; ν_{sym}(N-O), 1350; ν_{def}(O-N-O), 804; ν(C = C), 1579 s; ν(C = C) + ν (C = N)/pz ring, 1553 s, 1469 s; ν(C-S), 688 w; ν(ClO_4^-), 1106 br; δ(O–Cl–O), 623 s. UV-Vis spectra: λ_{max}/nm (ε_{max}/$mol^{-1}cm^{-1}$). 650 (73), 282 (3341), 251 (7834), 223 (14694). Λ_M ($\Omega^{-1}cm^2\,mol^{-1}$) = 119. μ_{eff} =1.78

3(B).2.2.4. Synthesis of [Cu(bdmpe)(NO_2)]PF_6 (4)

This complex was prepared by following the same procedure as that of complex **2**, however KNCS has been substituted with $NaNO_2$.

Yield. 0.117 g (75%). Found C = 38.42, H = 4.42, N = 13.14%. Anal calc for $C_{20}H_{27}CuF_6N_6O_2PS$: C = 38.49, H = 4.36, N = 13.47%. IR (KBr pellet) cm^{-1}: ν_{asym}(N-

O), 1381;ν_{sym}(N-O), 1350; ν_{def}(O-N-O), 804; ν(C = C), 1579 s; ν(C = C) + ν (C = N)/pz ring, 1553 s, 1469 s; ν(C-S), 688 w; ν(PF_6^-), 839 s. UV-Vis spectra: λ_{max}/nm (ε_{max}/$mol^{-1}cm^{-1}$). 657(179), 284 (3739), 251 (8545), 220 (19571). Λ_M ($\Omega^{-1}cm^2$ mol^{-1}) = 126. μ_{eff} = 1.77.

3(B).2.2.5. Synthesis of [Co(bdmpe)(NCS)$_2$] (5)

This complex was prepared by following the same procedure as that of complex **1**, however, $Cu(ClO_4)_2.6H_2O$ has been substituted with $Co(ClO_4)_2.6H_2O$.

Yield. 0.107 g (79%). Found C = 48.88, H = 5.08, N = 18.17%. Anal calc for $C_{22}H_{27}CoN_7S_3$: C = 48.52, H = 5.00, N = 18.00%. IR (KBr pellet) cm^{-1}: ν(NCS^-), 2078, 2063; ν(C = C), 1585 s; ν(C = C) +ν (C = N)/pz ring, 1552 s, 1468 s; ν(C-S), 644 w. UV-Vis spectra: λ_{max}/nm (ε_{max}/$mol^{-1}cm^{-1}$). 802 (37), 583(367), 490 (1390), 283 (4064), 250 (11832), 221 (21645). Λ_M ($\Omega^{-1}cm^2mol^{-1}$) = 13. μ_{eff} = 4.32 BM.

3(B).2.2.6. Synthesis of [Co(bdmpe)(N$_3$)]$_2$(ClO$_4$)$_2$ (6)

This complex was prepared by following the same procedure as that of complex **1**, however, $Cu(ClO_4)_2.6H_2O$ and KNCS have been substituted with $Co(ClO_4)_2.6H_2O$ and NaN_3.

Yield. 0.063 g (43%). Found C = 42.28, H = 4.80, N = 19.41%, Anal calc for $C_{40}H_{54}Cl_2Co_2N_{16}O_8S_2$: C = 42.15, H = 4.78, N = 19.66 %. IR (KBr pellet) cm^{-1}: ν(N_3^-), 2192; ν(C = C), 1576 s; ν(C = C) + ν (C = N)/pz ring, 1552 s, 1468 s; ν(C-S), 655 w; ν(ClO_4^-), 1096 br; δ(O–Cl–O), 623 s. UV-Vis spectra: λ_{max}/nm (ε_{max}/$mol^{-1}cm^{-1}$). 644 (68), 535 (115), 462 (183), 248 (13869), 221 (22349). Λ_M ($\Omega^{-1}cm^2$ mol^{-1}) = 122. μ_{eff} = 4.26 BM.

3(B).2.2.7. Synthesis of [Co(bdmpe)(N$_3$)]$_2$(PF$_6$)$_2$ (7)

This complex was prepared by following the same procedure as that of complex **2**, however, $Cu(ClO_4)_2.6H_2O$ and KNCS have been substituted with $Co(ClO_4)_2.6H_2O$ and NaN_3.

Yield. 0.073 g (47%). Found C = 39.12, H = 4.54, N = 18.46%. Anal calc for $C_{40}H_{54}Co_2F_{12}N_{16}P_2S_2$: C = 39.03, H = 4.42, N = 18.21%. IR (KBr pellet) cm^{-1}: ν(N_3^-), 2192; ν(C = C), 1576 s; ν(C = C) + ν (C = N)/pz ring, 1552 s, 1468 s; ν(C-S), 655 w;

$\nu(PF_6^-)$, 839 s. UV-Vis spectra: λ_{max}/nm (ε_{max}/mol^{-1}cm^{-1}). 645 (90), 533 (196), 461 (254), 250 (18246), 221 (25694). Λ_M (Ω^{-1}cm^2 mol^{-1}) = 119. μ_{eff} = 4.18.

3(B).3. X-ray Crystallography

Suitable size crystals of complexes **1**, **3, 5** and **6** [crystal size: **1**, 0.20 × 0.17 × 0.12 mm; **3**, 0.22 × 0.17 × 0.11 mm; **5**, 0.28 × 0.18 × 0.14mm; **6**, 0.28 × 0.18 × 0.13mm] were obtained by slow evaporation of methanol solution. Structure measurement performed on Oxford X-CALIBUR-S diffractometer equipped with two dimensional area CCD detector. The graphite monochromatized Cu-K_α radiation (λ = 1.541841Å) at 110 K for complexes **1** and with Mo-K_α radiation (λ = 0.71073Å) at 293 K for complexes **3, 5** and **6**, respectively and the ω-scan technique were used for data collection. The data interpretations were processed with CrysAlisPro, Agilent Technologies, Version 1.171.35.19 [26]. Absorption corrections were applied based on multi-scan method [27]. The structures were solved by direct methods and refined by the full-matrix least-square method based on F^2 technique using SHELXL-97 program package [28]. At convergence, the final residual were R1 = 0.0394(for complex **1**), 0.0594(for complex **3**), 0.0412(for complex **5**) and 0.0635(for complex **6**); R2 = 0.1025(for complex **1**), 0.1541(for complex **3**), 0.1017(for complex **5**) and 0.1719(for complex **6**) with I >2σ (I), goodness of fit = 0.611(**1**), 1.048(**3**), 0.990(**5**) and 1.038 (**6**), respectively. The final differences Fourier map showed the maximum and minimum peak heights of 0.58 and -0.34 eA^{-3} for **1**, 1.08 and -0.52 eA^{-3} for **3,** 0.71 and -0.74 eA^{-3} for **5**, and 0.96 and -0.44 eA^{-3} for **6**. All calculations were carried out using WinGX system Ver-1.64 crystallographic software [29]. All non-hydrogen atoms were refined anisotropic thermal parameter. All the hydrogen atoms attached to the carbon atoms were calculated from the difference Fourier map and treated as riding on the atoms to which they are attached. The crystal parameters, data collection and refinement results are summarized in Table 3(B).1 with selected bond length and angles listed in Table 3(B).2.

Table 3(B).1. Crystal parameters of complexes **1, 3, 5** and **6.**

	[Cu(bdmpe)(NCS)]ClO_4 (1)	**[Cu(bdmpe)(NO_2)]ClO_4 (3)**	**[Co(bdmpe)$(NCS)_2$] (5)**	**[Co(bdmpe)($\mu_{1,1}$-N_3)]$_2$(ClO_4)$_2$ (6)**
Empirical formula	$C_{44}H_{54}Cl_2Cu_2N_{10}O_8S_4$	$C_{20}H_{27}ClCuN_6O_6S$	$C_{22}H_{27}ClCoN_7OS_3$	$C_{40}H_{54}Cl_2Co_2N_{16}O_8S_2$
Formula weight	590.61	578.54	544.64	1139.87
Temperature (K)	110(13)	293(2)	293(2)	293(2)
Radiation	Cu Kα (λ = 1.54184)	Mo Kα (λ = 0.71073)	Mo Kα (λ = 0.71073)	Cu Kα (λ = 1.54184)
Crystal system	orthorhombic	monoclinic	triclinic	triclinic
Space group	$P2_12_12_1$	$P2_1/c$	*P-1*	*P-1*
a (Å)	12.20682(13)	7.4837(4)	8.300(5)	9.4423(7)
b (Å)	15.36602(13)	13.7085(7)	9.285(5)	11.0454(6)
c (Å)	27.1362(3)	24.8422(12)	17.951(5)	13.7349(9)
α, (°)	90	90	90.309(5)	75.197(5)
β(°)	90	94.511(5)	103.127(5)	70.029(7)
γ (°)	90	90	105.239(5)	73.790(6)
Volume (Å^3)	5089.95(9)	2540.7(2)	1296.8(11)	1272.29(16)
Z	4	4	2	1
Density (g cm^{-3})	1.5413	1.5124	1.3948	1.4876

Absorption coefficient (mm^{-1})	4.057	1.094	0.927	7.392
F(000)	2440.0	1196.0	567.5	590.0
θ range for data collection (°)	6.62 to 146.34	6.14 to 58	2.34 to 58.36	6.96 to 146.86
Index ranges	$-15 \le h \le 14$, $-10 \le k \le 19$, $-33 \le l \le 33$	$-10 \le h \le 9$, $-15 \le k \le 18$, $-32 \le l \le 31$	$-10 \le h \le 11$, $-12 \le k \le 12$, $-24 \le l \le 24$	$-11 \le h \le 11$, $-13 \le k \le 13$, $-17 \le l \le 17$
Reflections collected	21401	14979	23196	12796
Independent reflections	10198 [R_{int} = 0.0356, R_{sigma} = 0.0399]	6758 [R_{int} = 0.0262, R_{sigma} = 0.0365]	7028 [R_{int} = 0.0330, R_{sigma} = 0.0439]	5131 [R_{int} = 0.0501, R_{sigma} = 0.0476]
Data / restraints / parameters	10198/0/638	6758/0/319	7028/0/301	5131/0/319
Goodness-of-fit on F^2	0.611	1.048	0.990	1.038
Final R indices [*I*>2sigma(*I*)]	R_1 = 0.0394, wR_2 = 0.1025	R_1 = 0.0594, wR_2 = 0.1541	R_1 = 0.0412, wR_2 = 0.1017	R_1 = 0.0635, wR_2 = 0.1719
R indices (all data)	R_1 = 0.0402, wR_2 = 0.1037	R_1 = 0.0845, wR_2 = 0.1727	R_1 = 0.0783, wR_2 = 0.1254	R_1 = 0.0933, wR_2 = 0.1940
Largest diff. peak and hole (eA^{-3})	0.58 and -0.34	1.08 and -0.52	0.71 and -0.74	0.96 and -0.44
CCDC number	1545507	1545508	1545509	1545510

3(B).4. Results and Discussion

3(B).4.1. Syntheses

Four penta coordination mononuclear NCS^- and NO_2^- ion containing copper(II) complexes with general formula [Cu(bdmpe)(X)]Y, one mononuclear cobalt(II) complex $[Co(bdmpe)(NCS)_2]$ and two binuclear cobalt(II) complexes with general composition $[Co(bdmpe)(N_3)]_2(Y)_2$ [X = NCS^-, NO_2^- and Y = ClO_4^-, PF_6^-] were synthesized with good yield by mixing appropriate mole ratio of metal perchlorate/ nitrate, ligand bdmpe, coligand NCS^- / NO_2^- / N_3^- ions and NH_4PF_6 in methanol solution at ambient temperature (Scheme 3(B).1).

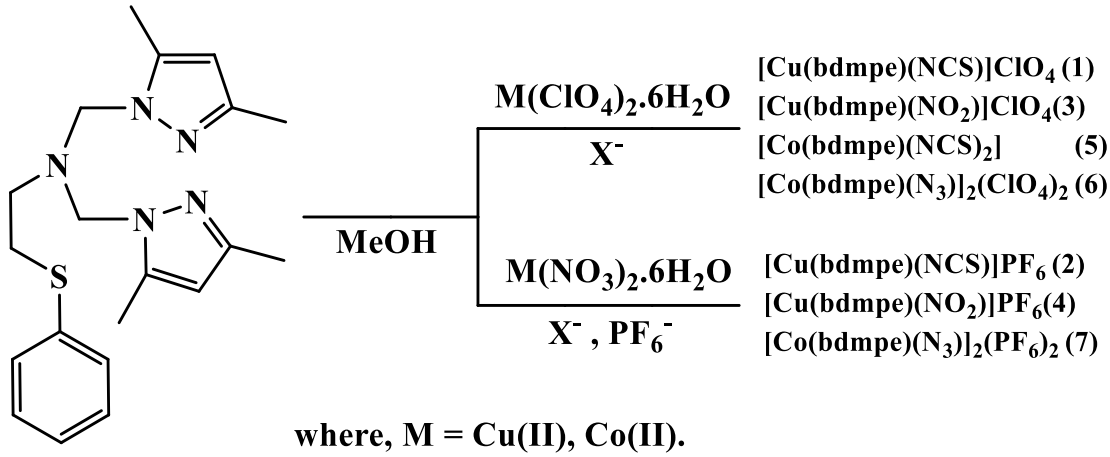

Scheme 3(B).1. Synthesis of complexes.

The molecular composition of the complexes are confirmed by microanalysis, solution conductivity, spectral data and finally by single crystal X-ray diffraction studies. Molar conductivity measurements in CH_3CN solution observed 1:1 electrolyte (Λ_M ~ 120 $\Omega^{-1}cm^2mol^{-1}$) for mononuclear copper(II) and binuclear cobalt(II) complexes indicating the presence of counter anion as secondary valence in complexes whereas mononuclear cobalt complex behave as non-electrolytes (Λ_M ~ 10 $\Omega^{-1}cm^2$ mol^{-1}) indicating no counter anion in the molecule [30]. The conductivity of all complexes remain constant after 3 h indicating no dissociation of the complexes in the solution. The presence of the counter anion was also proved by IR spectra and single crystal X-ray diffraction studies. Based on this data, it can be concluded that all complexes are mononuclear except azide containing cobalt(II) complexes and ligand bdmpe coordinated to all complexes through four coordination sites but in

mononuclear cobalt(II) complex it behave as a tridentate with N_3-coordination. Synthesis of copper(II) complexes with azide and cobalt(II) complexes with NO_2 co-ligand complexes were unsuccessful. All the complexes are stable in air and well soluble in common organic solvents such as acetonitrile, methylene chloride, DMF etc sparingly soluble in MeOH, EtOH and poorly soluble in H_2O.

3(B).4.2. IR, UV-Visible spectra, EPR and magnetic spectral data

3(B).4.2.1. IR data

The important bands of IR spectra of all synthesized complexes with their assignments are reported in section 3(B).2.2. The IR spectrum of the ligand bdmpe and all the synthesized complexes exhibit common absorption bands at ~ 1576 cm^{-1} for *ν*(C=C) of the phenyl rings, at ~ 1553 and ~ 1467 cm^{-1} due to *ν*(C=N) + *ν*(C=C) of the pyrazole ring and at ~ 656 cm^{-1} for *ν*(C-S) of thioether, indicating the co-ordination of the pyrazole groups and sulphur atom of ligand bdmpe to the metal centre in the complexes. The binding mode of NCS^- anion to the metal ions is detected by the strong IR band due to NCS^- ion which occurs above 2000 cm^{-1}. The CN stretching vibration for N-bonded SCN^- usually appears below 2100 cm^{-1} and that of S-bonded thiocyanate appear above 2100 cm^{-1} [31-32]. The complexes **1** and **2** show one intense band at ~ 2094 cm^{-1} and complex **5** show two intense bands at 2078 and 2063 cm^{-1} indicating the presence of N-bonded thiocyanate group in the complexes. Complexes **3** and **4** exhibit N-O asymmetric starching at 1381 cm^{-1} and a symmetric a stretch at 1350 cm^{-1}. The O-N-O deformation band observed at 804 cm^{-1} [33-34]. Complexes **6** and **7** show two strong bands in the region of 2045-2059 cm^{-1} indicating end-on bridging coordination modes of the two azide ions. In general, the end-on bridging vibration of the azide (N_3^-) ion appears at 2060-2070 cm^{-1} whereas the end-to-end bridging mode appears at 2020-2040 cm^{-1} [35]. The IR spectra of complexes **1**, **3** and **6** exhibited two bands: one broad band at ~ 1100 cm^{-1} due to ν_{asmy}(Cl-O) and a band at ~ 623 cm^{-1} due to δ(O-Cl-O), confirming the presence of perchlorate ion outside the coordination sphere in the complexes. Similarly, one strong band at ~ 844 cm^{-1} due to *ν*(PF_6^-) indicating the presence of counter anion of complexes **2**, **4** and **7**. For complexes **4** and **5** no bands was observed at 1100 or 623 cm^{-1} indicating the absence of ClO_4^- as counter anion in the complexes and the molecule is non-ionic in nature [36].

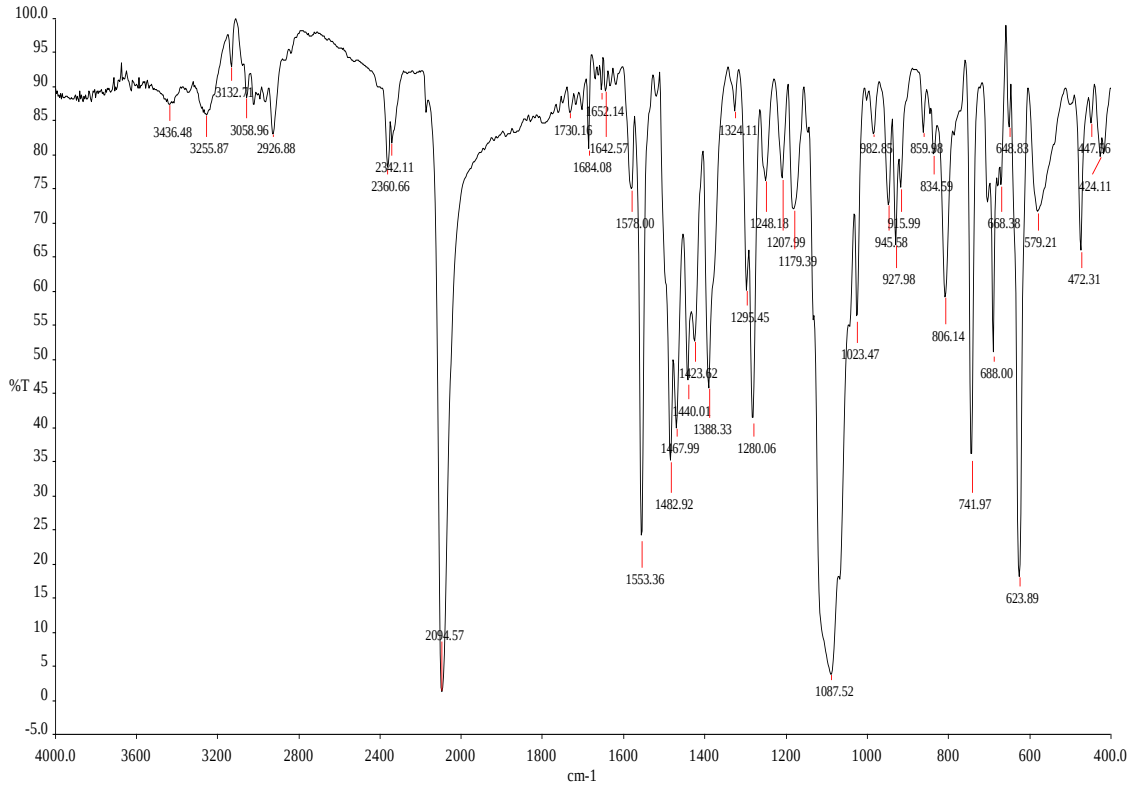

Fig.3(B).1. IR spectrum of $[Cu(bdmpe)(NCS)]ClO_4$ (**1**).

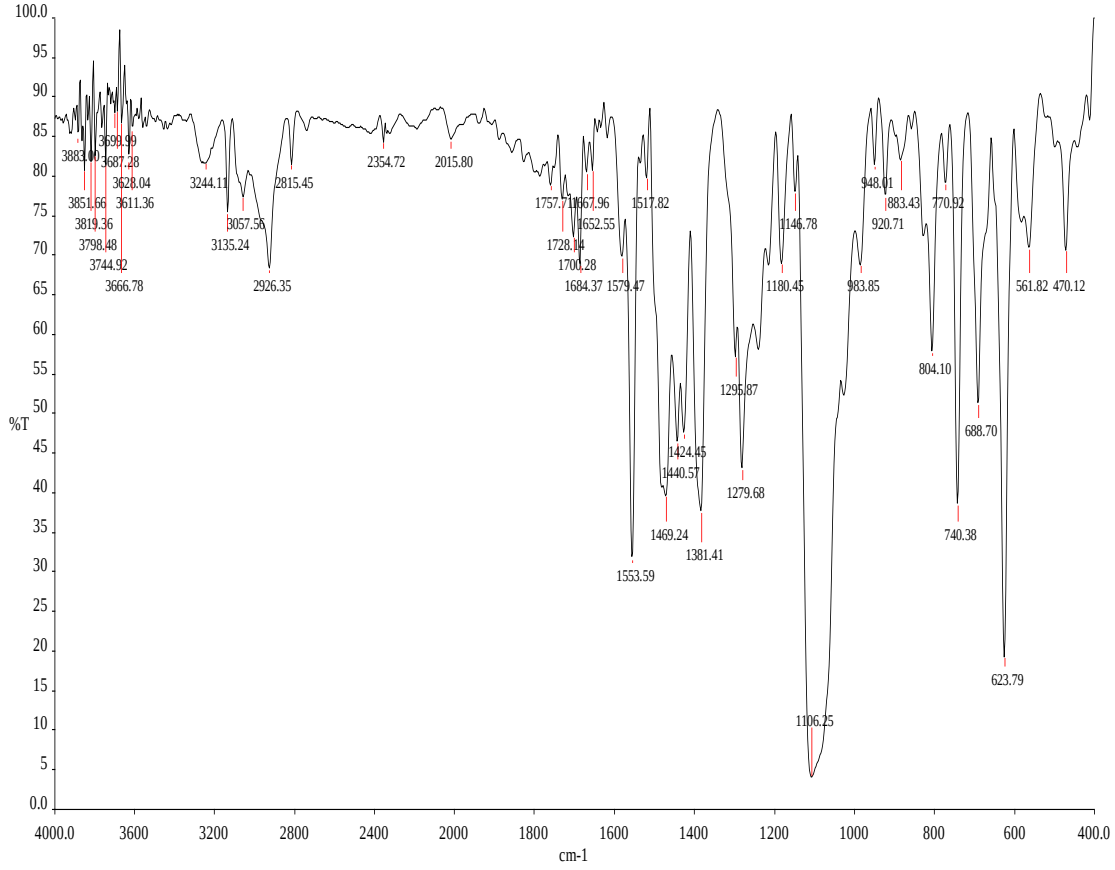

Fig.3(B).2. IR spectrum of $[Cu(bdmpe)(NO_2)]ClO_4$ (**3**).

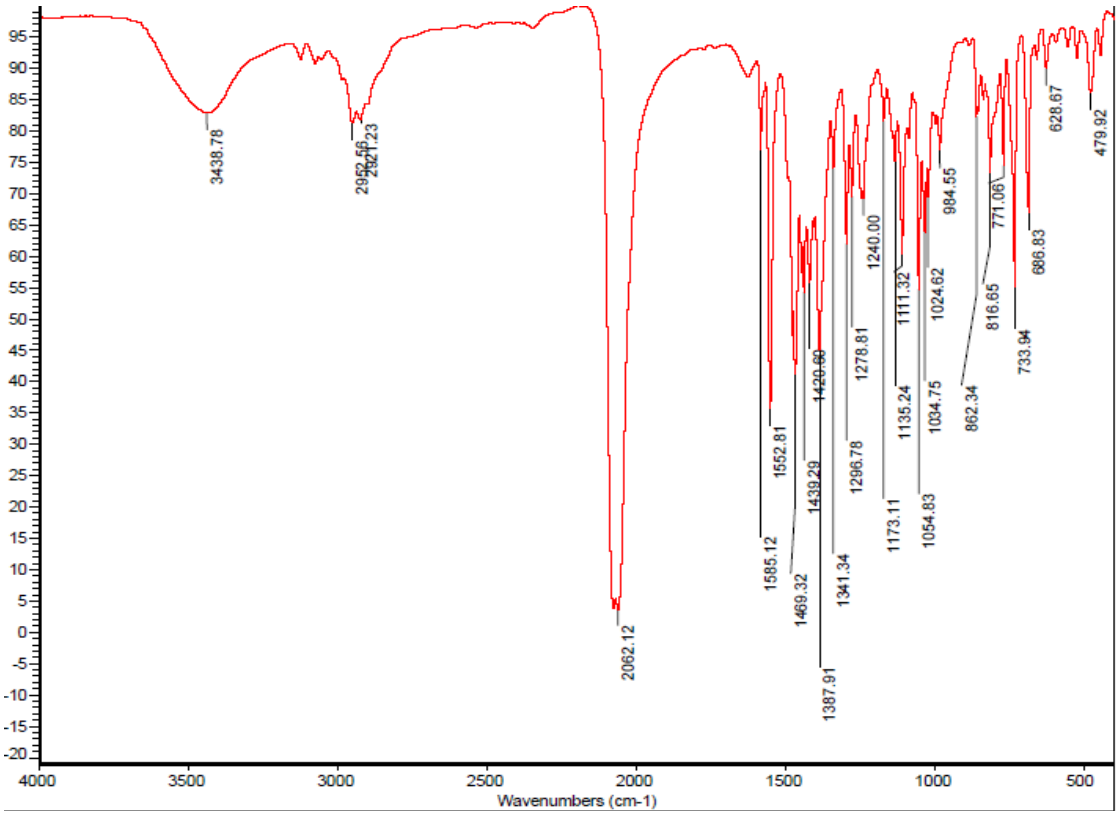

Fig.3(B).3. IR spectrum of $[Co(bdmpe)(NCS)]_2$ (**5**).

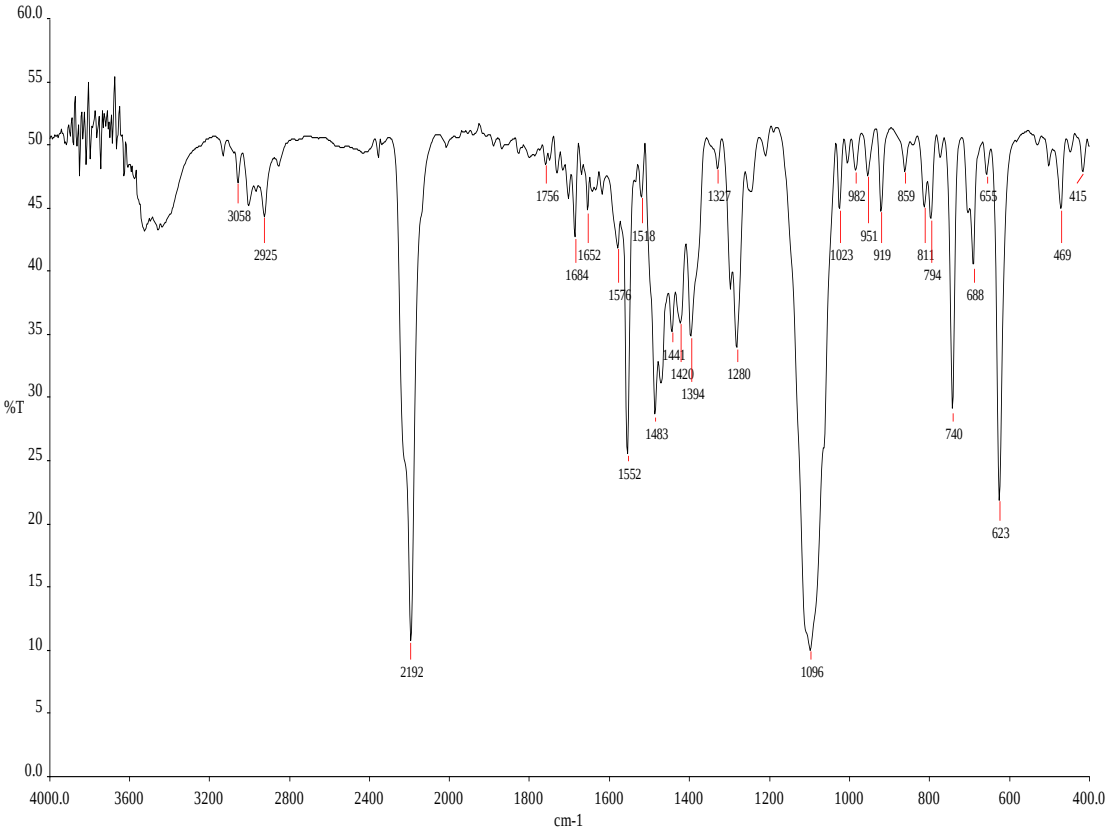

Fig.3(B).4. IR spectrum of $[Co(bdmpe)(N_3)]_2(ClO_4)_2$ (**6**).

3(B).4.2.2. UV-Visible spectra, EPR and magnetic data

The electronic spectra of ligand and their complexes were drawn in CH_3CN (10^{-3} M) in the range of 200-1100 nm. The high intensity bands appeared at < 400 nm is due to intra ligand charge transfer transition. For copper (II) complexes, all complexes show one absorption band at ~ 661 nm with molar excitation coefficient ~ 180 $mol^{-1}cm^{-1}$ and it may be due to d_{xz}, $d_{yz} \rightarrow d_{x^2-y^2}$ transition. Most of the reported Cu(II) complexes with square pyramidal or distorted square pyramidal geometry show spectral band in the region of 550-660 nm due to the above transition. [37-38]. For complex **5**, there are three bands in the visible region at 802, 583 and 490 nm and these are due to $^4A_2'(F) \rightarrow {}^4E'(F)$, $^4A_2'(F) \rightarrow {}^4E''(P)$ and $^4A_2'(F) \rightarrow {}^4A_2'(P)$ transition respectively. Cobalt(II) complexes with trigonal bipyramidal geometry shows this type transitions [39]. Complex **6** and **7** show three d-d transition around at ~644, ~535 and ~462 nm, respectively. This type of transitions are generally observed for cobalt(II) complexes with octahedral geometry [40].

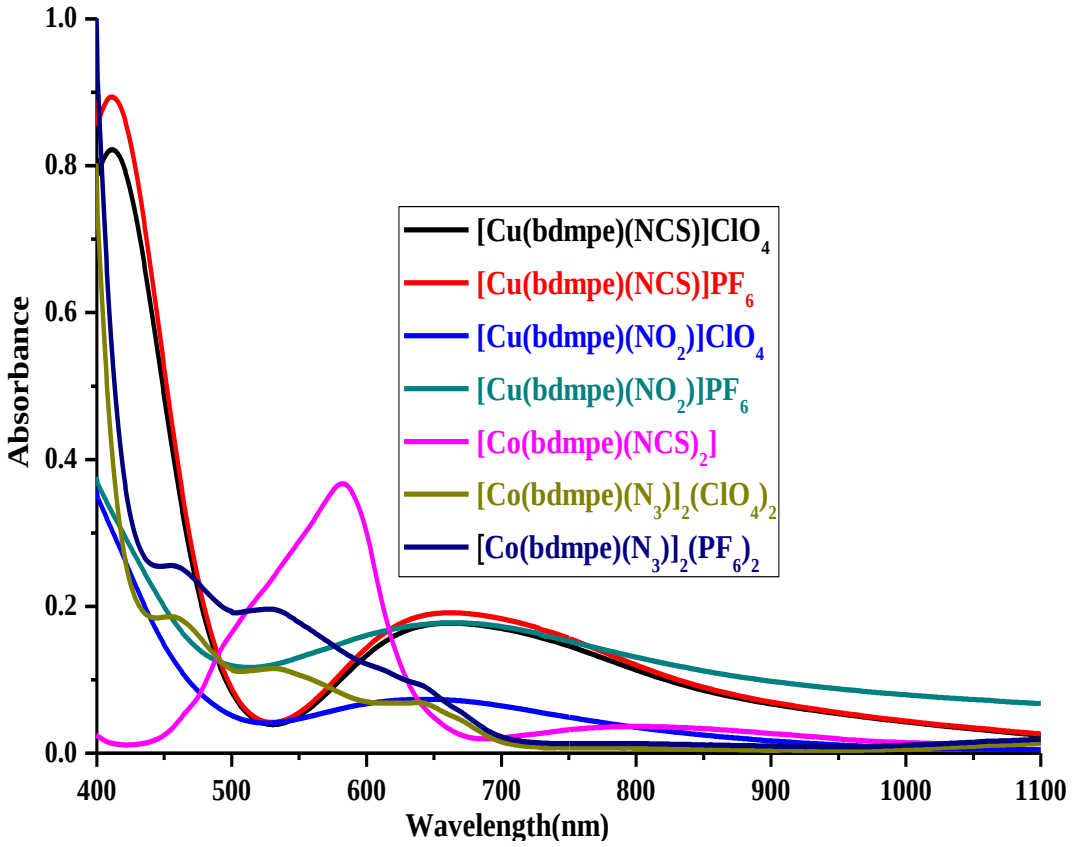

Fig.3(B).5. UV-Visible spectra of the complexes in CH_3CN solution (10^{-3} M).

The X-band EPR spectra of the complexes **1** and **3** in frozen DMF solution (77 K) show four-line spectrum characteristic of mononuclear copper(II) complexes with d^9 configuration (s = 1/2). Spectral data showed that g_{II} = 2.271 and $g_{\perp}$ = 2.057 for complex **1** and with g_{II} = 2.263 and $g_{\perp}$ = 2.053 for complex **3**, indicating the interaction of the unpaired electron with nuclear spin of the copper(II) nucleus (^{63,65}Cu; I = 3/2). The g_{II} value is greater than $g_{\perp}$ indicating a pseudotetragonal site symmetry of the copper(II) in the complexes and similar g_{II} and $g_{\perp}$ values for both the complexes indicate the similar structure of the complexes.

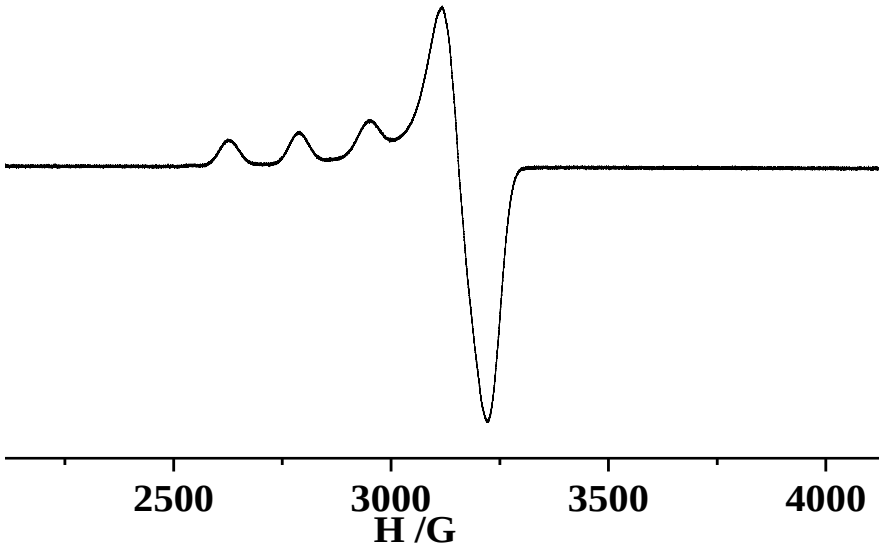

Fig.3(B).6. X-Band EPR spectrum of complex **1** in DMF solution at 77 K.

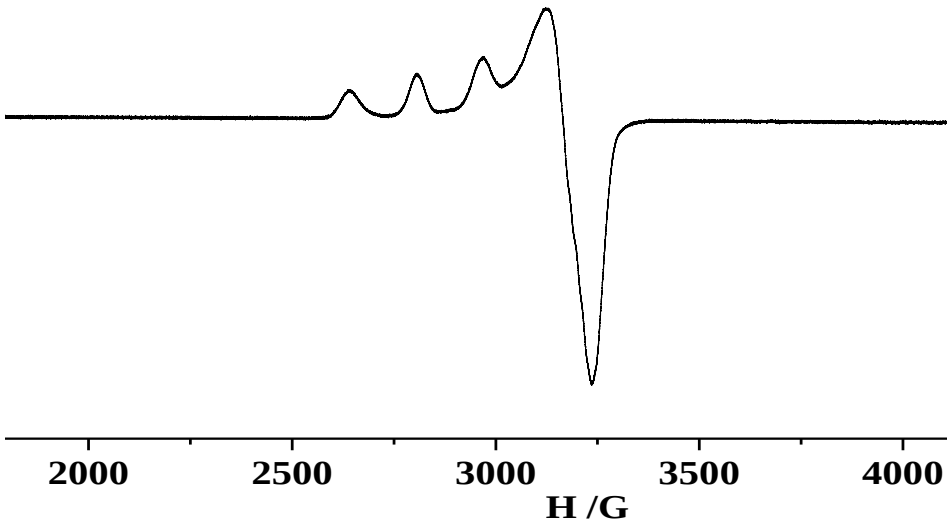

Fig.3(B).7. X-Band EPR spectrum of complex **3** in DMF solution at 77 K.

The magnetic susceptibility measurements in the solid state show that all the complexes are paramagnetic in nature. The effective magnetic moment (μ_{eff}) of the copper(II) complexes at room temperature is ~ 1.78 B.M corresponding to one unpaired electron and for the cobalt(II) complexes, the magnetic moment ~ 4.32 B.M at room temperature supporting to three unpaired electrons. The observed magnetic moment values of these complexes are close to the spin only value. Generally magnetic moment of cobalt(II) complexes with tripodal ligand are shown in this region [41-43].

3(B).4.3. Description of Crystal Structures

3(B).4.3.1. Crystal structures of [Cu(bdmpe)(X)]ClO_4 [X = NCS(1), NO_2(3)]

ORTEP diagrams of [Cu(bdmpe)(NCS)]ClO_4 and [Cu(bdmpe)(NO_2)]ClO_4 complexes with the atomic labeling scheme are shown in Fig.3(B).8 and 9, respectively. Structure refinement parameters and crystal data for both complexes are summarized in Table 3(B).1 and relevant interatomic bond distances and angles are summarized in Table 3(B).2. The unit cell contains $[Cu(bdmpe)(X)]^+$ mononuclear unit isolated by perchlorate counter anion for both complexes. Single crystal X-ray analysis revealed that the complex **1** is mononuclear crystallizes in orthorhombic lattice with $P2_12_12_1$ chiral space group symmetry with four molecules in an unit cell and mononuclear complex **3** crystallizes in monoclinic lattice with $P2_1/c$ space group symmetry with four molecules in an unit cell. The copper(II) ion of both complexes are five coordinated - four of them surrounded by two pyrazoyle nitrogen, one tertiary nitrogen and one sulfur atom of ligand bdmpe and remaining position is occupied by thiocyanate nitrogen or nitrite oxygen, respectively.

For complex **1**, the τ value [Addison structural index parameter $\tau = (\beta - \alpha)/60$), where α = 162.42(11)º (N(1)-Cu(1)-N(5)) and β = 170.37(12)º (N(6)-Cu(1)-N(3))] is 0.17, therefore, the geometry of copper(II) center is slightly distorted square pyramidal [44]. Copper(II) center is surrounded by the four nitrogen atoms- one nitrogen atom N(6) from NCS ion, two from set of pyrazole group N(1), N(5) and one from tertiary nitrogen N(3) consisting of ligand bdmpe and the three equatorial bond distances Cu(1)-N(6) [1.935(3)Å], Cu(1)-N(1) [1.973(3)Å] and Cu(1)-N(5) [1.956(3)Å] are nearly equal but shorter than Cu(1)-N(3) [2.103(3)Å] distance.

Table 3(B).2. Important Bond lengths (Å) and bond angels (°) of complexes **1**, **3**, **5** and **6.**

Bond lengths (Å)							
[Cu(bdmpe)(NCS)]ClO_4 (1)		**[Cu(bdmpe)(NO_2)]ClO_4 (3)**		**[Co(bdmpe)$(NCS)_2$] (5)**		**[Co(bdmpe)($\mu_{1,1}$-N_3)]$_2$(ClO_4)$_2$ (6)**	
Cu(1)-S(1)	2.7165(9)	Cu(1)-N(3)	2.117(3)	Co(1)-N(3)	2.412(2)	Co(1)-S(1)	2.5741(14)
Cu(1)-N(5)	1.956(3)	Cu(1)-N(1)	1.965(3)	Co(1)-N(5)	2.058(2)	Co(1)-N(6)	2.083(4)
Cu(1)-N(3)	2.103(3)	Cu(1)-N(5)	1.969(3)	Co(1)-N(1)	2.033(2)	Co(1)-N(6i)	2.172(4)
Cu(1)-N(6)	1.935(3)	Cu(1)-O(1)	1.956(3)	Co(1)-N(6)	2.000(3)	Co(1)-N(3)	2.232(4)
Cu(1)-N(1)	1.973(3)	Cu(1)-S(1)	2.7171(11)	Co(1)-N(7)	1.978(3)	Co(1)-N(4)	2.102(4)
						Co(1)-N(1)	2.100(4)

Bond angels (°) of complexes **1**, **3**, **5** and **6.**

Bond angles (°)							
[Cu(bdmpe)(NCS)]ClO_4 (1)		**[Cu(bdmpe)(NO_2)]ClO_4 (3)**		**[Co(bdmpe)$(NCS)_2$] (5)**		**[Co(bdmpe)($\mu_{1,1}$-N_3)]$_2$(ClO_4)$_2$ (6)**	
N(5)-Cu(1)-S(1)	93.57(8)	N(1)-Cu(1)-N(3)	82.35(12)	N(5)-Co(1)-N(3)	73.94(7)	N(6)-Co(1)-S(1)	96.88(12)
N(3)-Cu(1)-S(1)	84.09(8)	N(5)-Cu(1)-N(3)	81.83(12)	N(1)-Co(1)-N(3)	74.58(7)	N(6i)-Co(1)-S(1)	171.87(12)
N(3)-Cu(1)-N(5)	81.69(11)	N(5)-Cu(1)-N(1)	163.29(13)	N(1)-Co(1)-N(5)	113.06(8)	N(3)-Co(1)-S(1)	84.75(11)
N(6)-Cu(1)-S(1)	105.47(9)	O(1)-Cu(1)-N(3)	166.58(14)	N(3)-Co(1)-N(6)	175.44(8)	N(3)-Co(1)-N(6i)	97.81(15)
N(6)-Cu(1)-N(5)	98.59(12)	O(1)-Cu(1)-N(1)	97.32(14)	N(6)-Co(1)-N(5)	101.50(9)	N(3)-Co(1)-N(6)	178.28(16)
N(6)-Cu(1)-N(3)	170.37(12)	O(1)-Cu(1)-N(5)	96.81(14)	N(6)-Co(1)-N(1)	107.68(9)	N(4)-Co(1)-S(1)	93.33(12)
N(1)-Cu(1)-S(1)	89.19(8)	N(3)-Cu(1)-S(1)	82.85(9)	N(7)-Co(1)-N(3)	86.40(8)	N(4)-Co(1)-N(6)	104.11(16)
N(1)-Cu(1)-N(5)	162.42(11)	N(1)-Cu(1)-S(1)	93.85(10)	N(7)-Co(1)-N(5)	124.20(8)	N(4)-Co(1)-N(6i)	94.77(16)
N(3)-Cu(1)-N(1)	81.34(11)	N(5)-Cu(1)-S(1))	89.51(10)	N(7)-Co(1)-N(1)	110.74(10)	N(4)-Co(1)-N(3)	76.32(16)
N(6)-Cu(1)-N(1)	97.38(12)	O(1)-Cu(1)-S(1)	110.52(12)	N(7)-Co(1)-N(6)	96.35(10)	N(1)-Co(1)-S(1)	80.20(13)
						N(1)-Co(1)-N(6)	102.69(17)
						N(1)-Co(1)-N(6i)	92.82(16)
						N(1)-Co(1)-N(3)	76.99(16)
						N(4)-Co(1)-N(1)	153.00(17)

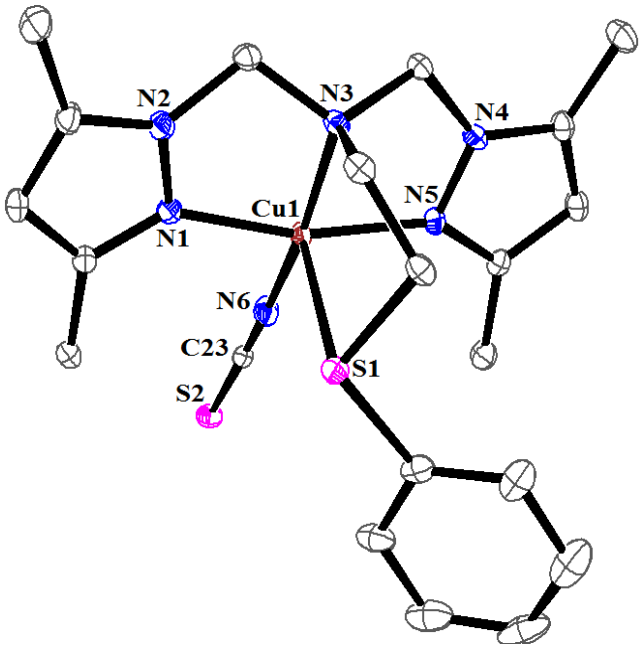

Fig.3(B).8. ORTEP diagram depicting the cationic part of the complex [Cu(bdmpe)(NCS)]ClO_4 (**1**) with atom numbering scheme (40% probability factor for the thermal ellipsoids).

The apical position of the square pyramid geometry is occupied by sulfur atom S(1) from ligand bdmpe and the distance Cu(1)-S(1) is 2.7165(9) Å. As expected, the Cu-S distance at the apical position is slightly longer than the equatorial Cu-N distances which may be due to the Jahn-Teller effect of Cu(II) center. The copper atom located at a distance 0.146 Å above the CuN_4 coordination plane towards to the axially coordinated thiophenyl sulfur. The selected angles between metal and coordination sphere are: N(1)-Cu(1)-S(1) = 89.19(8)º, N(3)-Cu(1)-S(1) = 84.09(8)º, N(5)-Cu(1)-S(1) = 93.57(8)º, N(6)-Cu(1)-S(1) = 105.47(9)º, N(6)-Cu(1)-N(3)= 170.37(12)º and N(1)-Cu(1)-N(5) = 162.42(11)º. The terminal NCS ion is nearly linear to the copper(II) center with N(6)-C(23)-S(2) 178.93(3)º bond angle. The neutral ligand bdmpe coordinate to the cobalt center and formed three sets of five member chelate rings and their chelate intra ligand bite angles are 81.34(11)º [N(1)–Cu(1)–N(3)], 81.69(11)º [N(3)–Cu(1)–N(5)] and 84.09(8)º, [N(3)–Cu(1)–S(1)]. The bond lengths and angles are comparable with reported five coordinated mononuclear copper(II) complexes with tetradentate tripodal N_3S-coordinated ligand [45-47].

For complex **3**, the τ value is equal to 0.05 [τ =(β - α)/60), where α = 163.29(13)º [N(5)-Cu(1)-N(1)] and β = 166.58(14)º [O(1)-Cu(1)-N(3)], therefore, the geometry of copper(II) center is best described as slightly distorted square based pyramidal. The equatorial position around copper(II) center is surrounded by the three nitrogen atoms- two nitrogen atoms N(1), N(5) from set of pyrazole groups and one nitrogen atom N(3) from tertiary nitrogen consisting of ligand bdmpe and one oxygen atom O(1), from NO_2 group and the three equatorial bond distances Cu(1)-O(1) [1.956(3)Å], Cu(1)-N(1) [1.965(3)Å] and Cu(1)-N(5) [1.969(3)Å] are equal but different from the fourth Cu(1)-N(3) [2.117(3)Å] distance. The apical position of the square pyramid geometry is occupied by sulfur atom S(1) from ligand bdmpe with long Cu-S [2.7171(11)Å] distance.

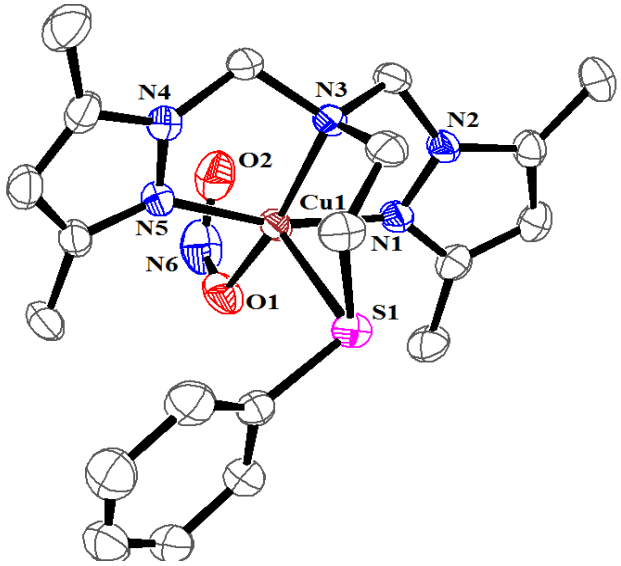

Fig.3(B).9. ORTEP diagram depicting the cationic part of the complex [Cu(bdmpe)(NO_2)]ClO_4 (**3**) with atom numbering scheme (40% probability factor for the thermal ellipsoids).

As expected, the Cu-S distance at the apical position is slightly longer than the bonds in the equatorial Cu-N distances or Cu-O distance and this may be due to the Jahn-Teller effect. The copper atom located at a distance 0.180 Å above the CuN_3O coordination plane towards to the axially coordinated thiophenyl sulfur. The selected angles between metal and coordination sphere are: N(1)-Cu(1)-S(1) = 93.85(10)º, N(3)-Cu(1)-S(1) = 82.85(9)º, N(5)-Cu(1)-S(1) = 89.51(10)º, O(1)-Cu(1)-S(1) = 110.52(12)º, O(1)-Cu(1)-N(3) = 166.58(14)º and N(1)-Cu(1)-N(5) = 163.29(13)º. The neutral ligand bdmpe coordinate to the copper center and forming

three sets of five membered chelate rings and and their chelate intra-ligand bite angle are 82.35(12)º [N(1)–Cu(1)–N(3)], 81.83(12)º [N(3)–Cu(1)–N(5)] and 82.85(9)º [N(3)–Cu(1)–S(1)]. The terminal NO_2 ion is not linear to the copper(II) center as the Cu(1)-O(1)-N(6) angle is 108.94(3)º and O-N-O bond angle is 115.0(5). The bond lengths and angles are comparable with reported five coordinated mononuclear copper(II) complexes with tetradentate tripodal N_3S-coordinated ligand [48-50].

3(B).4.3.2. Crystal structures of [Co(bdmpe)(NCS)$_2$] (5) and [Co(bdmpe)($\mu_{1,1}$-N_3)]$_2$(ClO_4)$_2$ (6)

ORTEP diagrams of the complex **5** [Co(bdmpe)$(NCS)_2$] and complex **6** [Co(bdmpe)($\mu_{1,1}$-N_3)]$_2$(ClO_4)$_2$, with the atomic labeling scheme are shown in Fig.3(B).10 and 11, respectively. The unit cell of complex **5** consists of neutral and mononuclear unit [Co(bdmpe)$(NCS)_2$] whereas complex **6** consist of [Co(bdmpe)($\mu_{1,1}$-N_3)]$^{+2}$ cations isolated by non-coordinating perchlorate counter anions. Single crystal X-ray analysis revealed that both the cobalt(II) complexes are crystallized in triclinic lattice with *P-1* space group.

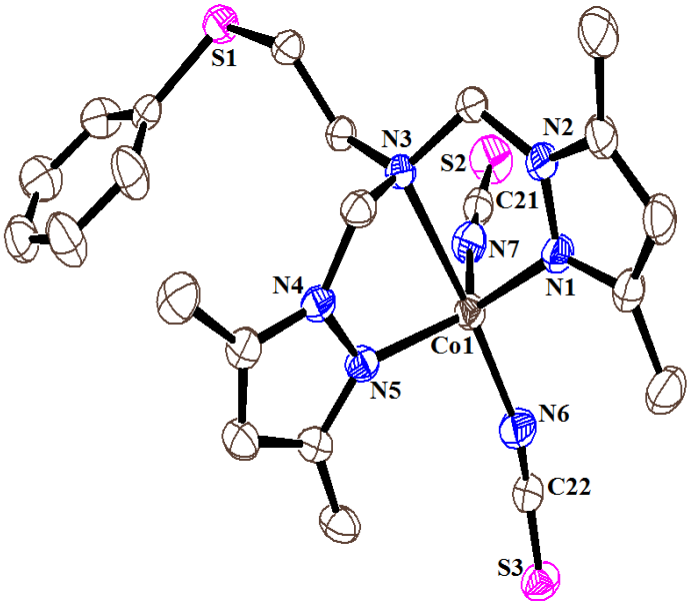

Fig.3(B).10. ORTEP diagram depicting the cationic part of the complex [Co(bdmpe)$(NCS)_2$] (**5**) with atom numbering scheme (40% probability factor for the thermal ellipsoids).

For complex **5**, the τ value is 0.85 indicating geometry of cobalt(II) center is best described as slightly distorted trigonal bipyramidal. So the cobalt center is

coordinated by five nitrogen donor atoms–three nitrogen atoms are coordinating from the ligand bdmpe and two nitrogen atoms from terminal NCS ions. Crystal structure of complex shows that the ligand bdmpe acts as N_3-coordinated tridentate ligand and sulfur atom of ligand bdmpe remain uncoordinated with copper center. So the geometry turns to SP from TBP. In the TBP environment, the basal plane around cobalt(II) center is surrounded by the three nitrogens: one nitrogen atom N(7) from NCS group and two from set of pyrazole groups N(1), N(5) of ligand bdmpe and the equatorial bond distances are Co(1)-N(7) =1.978(3)Å, Co(1)-N(1) = 2.033(2)Å and Co(1)-N(5) = 2.058(2)Å. The axial positions are occupied by two nitrogen atoms- one from tertiary nitrogen atom N(3) of ligand bdmpe and one nitrogen N(6) from another NCS group and the apical bond distance Co(1)-N(3) [2.412(2) Å] is longer than Co(1)-N(6) [2.000(3)Å]. The cobalt atom is located at a distance 0.407 Å above the equatorial CuN_3 plane towards to the axially coordinated N(6) nitrogen of NCS ligand. The selected equatorial bond angles between cobalt and coordination sphere are: N(1)-Co(1)-N(5) = 113.06(8)º, N(7)-Co(1)-N(5) = 124.20(8)º and N(7)-Co(1)-N(1) = 110.74(10)º. The axial bond angle N(7)-Co(1)-N(5) is 175.44(8)º and it deviates slightly from ideal 180º. The neutral ligand bdmpe has formed two sets of five member chelate rings and their chelate intra-ligand bite angles are 74.58(7) [N(1)–Co(1)–N(3)] and 73.94(7) [N(3)–Co(1)–N(5)]. Two terminal NCS ions are nearly linear and their bond angles are 179.0(3)º [N(6)–C(22)–S(3)] and 179.6(3)º [N(7)–C(21)–S(2)] but are bonded with cobalt centers with different bond angles 171.6(2)° [Co-N(7)-C(21)] and 164.4(2)° [Co-N(6)-C(22)]. The bond lengths and angles are comparable to similar type of compounds [51-53].

The complex **6** is binuclear in nature and the unit cell contains two centro-symmetric $[Co(bdmpe)(N_3)]^{2+}$ binuclear entities. Each cobalt(II) center has octahedral geometry and surrounded by six heteroatoms - two nitrogen atoms N(6), N(6i) from pair of bridging azide ligands, three nitrogen N(1), N(3), N(4) and one sulfur atom S(1) from ligand bdmpe. The axial positions are occupied by S(1) and N(6i) atoms with long Co-S(1) [2.5741(14)Å] bond distance than Co-N(6i) [2.172(4)Å] and the equatorial positions are occupied by N(1), N(3), N(4) and N(6) atoms and their distances from cobalt centers Co-N(1) [2.100(4) Å], Co-N(3) [2.232(4) Å], Co-N(4) [2.102(4) Å] and Co-N(6) [2.083(4)Å] are not equal.

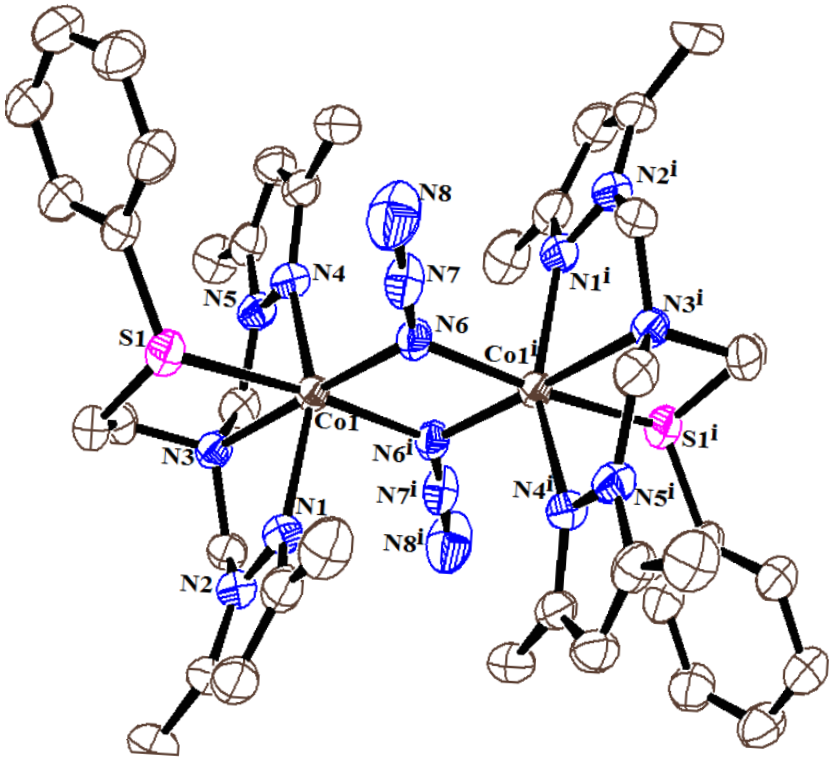

Fig.3(B).11. ORTEP diagram depicting the cationic part of the complex $[Co(bdmpe)(\mu_{1,1}\text{-}N_3)]_2(ClO_4)_2$ (**6**) with atom numbering scheme (40% probability factor for the thermal ellipsoids).

So the cobalt atom has distorted octahedral structure with short equatorial bond distances (<2.102 Å) and two much longer axial bonds (>2.172 Å). The bond lengths of Co(II)-N(azide) are comparable with other reported similar binuclear complexes [54]. The complex possess center of symmetry, so the coordination environment around Co(1) center is very similar to that of Co(1i) center. The crystal structure of the complex is also support that two azide ions bridged with two cobalt centers in double EO (μ-1,1) mode and formed four member planar Co_2N_2 ring. The bond angles of (μ-1,1) azido bridges with two cobalt centers are: Co(1)–N(6)–Co(1i) = 99.49(2)º, N(6)–N(7)–N(8) = 178.75(7)º, Co(1)–N(6)–N(7) = 132.41(4)º and Co(1i)–N(6)–N(7) = 126.32(4)º. The intradimer Co(1)….Co(1i) distance within the Co_2N_2 ring is 3.247 Å and this is consistent with structural data obtained with other reported binuclear end-on azide bridging complexes [55-56].

3(B).5. Conclusion

Tetradentate N_3S-donor ligand *N*,*N*-bis((3,5-dimethyl-1*H*-pyrazol-1-yl)methyl)-2-(phenylthio)ethan-1-amine (bdmpe) has been used for the synthesis of azide / thiocyanate / nitrite containing copper(II) and cobalt(II) complexes. The synthesized complexes were well characterized by microanalysis, IR, electronic spectral studies, magnetic studies and EPR spectral data including single crystal X-ray diffraction studies. Single crystal X-ray studies revealed that NCS, NO_2-containing mononuclear [Cu(bdmpe) $(NCS/NO_2)]ClO_4$ complexes have square pyramidal, NCS containing mononuclear $[Co(bdmpe)(NCS)_2]$ complex has trigonal bipyramid and end-on azido bridged binuclear $[Co(bdmpe)(N_3)]_2(ClO_4)_2$ complex has octahedral geometry. All complexes crystallized in achiral space group whereas complex $[Cu(bdmpe)(NCS)]ClO_4$ crystallized in chiral space group $P2_12_12_1$. Flexible ligand bdmpe behaves as tetradentate in all complexes except in complex $[Co(bdmpe)(NCS)_2]$ where it behave as tridentate and sulphur atom remain uncoordinated with cobalt centre.

3(B).5. References:

1. M.A.S. Goher, F.A. Mautner, M.A.M. Abu-Youssef, A.K. Hafez, A.M.A. Badr, J. Chem. Soc., Dalton Trans. (2002) 3309.
2. P. Chakraborty, S. Purkait, S. Mondal, A. Bauzá, A. Frontera, C. Massera, D. Das, Cryst. Eng. Comm. 17 (2015) 4680.
3. M.H. Sadhu, A. Solanki, T. Kundu, V. Hingu, B. Ganguly, S.B. Kumar Polyhedron 133 (2017) 8.
4. M.G. Sommer, R. Marx, D. Schweinfurth,Y. Rechkemmer, P. Neugebauer, M. van der Meer, S. Hohloch, S. Demeshko, F. Meyer, J. van Slageren, B. Sarkar, Inorg. Chem. 56 (2017)402.
5. A. Solanki, M. Monfort, S.B. Kumar, J. Mol. Struct. 1050 (2013) 197.
6. C. Diaz, J. Ribas, M.S. El Fallah, X. Solans, M. Font-Bardia, Inorg. Chim. Acta 312 (2001) 1.
7. M.H. Sadhu, A. Solanki, S.B. Kumar, Polyhedron 100 (2015) 206.
8. J. Vallejo, I. Castro, R. Ruiz-Garcia, J. Cano, M. Julve, F. Lloret, G. De Munno, W. Wernsdorfer, E. Pardo, J. Am. Chem. Soc. 134 (2012) 15704.
9. V. Thamilarasan, A. Jayamani, N. Sengottuvelan, Eur. J. Med. Chem. 89 (2015) 266.
10. M. Das, S. Chatterjee, S. Chattopadhyay, Polyhedron 68 (2014) 205.
11. M.H. Sadhu, S.B. Kumar, Polyhedron 123 (2017) 419.
12. J. Carranza, M. Julve, J. Sletten, Inorg. Chim. Acta 361 (2008) 2499.
13. S.S. Massoud, A.E. Guilbeau, H.T. Luong, R. Vicente, J.H. Albering, R.C. Fischer, F.A. Mautner, Polyhedron 54 (2013) 26.
14. F.A. Mautner, M. Scherzer, C. Berger, R.C. Fischer, R. Vicente, S.S. Massoud, Polyhedron 85 (2015) 20.
15. S. Mondal, P. Chakraborty, N. Aliaga-Alcalde, S. Mohanta, Polyhedron 63 (2013) 96.
16. F.A. Mautner, C. Berger, C. Gspan, B. Sudy, R.C. Fischer, S.S. Massoud, Polyhedron 130 (2017) 136.
17. P. Bhowmik, S. Chattopadhyay, M.G.B. Drew, A. Ghosh, Inorg. Chim. Acta 395 (2013) 24.
18. H. Grove, M. Julve, F. Lloret, P.E. Kruger, K.W. Törnroos, J. Sletten, Inorg. Chim. Acta 325 (2001) 115.

19. S.S. Massoud, F.R. Louka, R.N. David, M.J. Dartez, Q.L. Nguyn, N.J. Labry, R.C. Fischer, F.A. Mautner, Polyhedron 90 (2015) 258.
20. A. Solanki, M. Montfort, S.B. Kumar, J. Mol. Struct. 1050 (2013) 197.
21. C. Chen, H. Qiu, W. Chen, Inorg. Chem. 50 (2011) 8671.
22. J. Olguin, S. Brooker, Coord. Chem. Rev. 255 (2011) 203.
23. A.R. Katritzky, X. Yong-Jiang, H. Hai-Ying, S. Mehta, J. Org. Chem. 66 (2001) 5590.
24. W.L. Driessen, Recl. Trav. Chim. Pays-Bas. 101 (1982) 441.
25. M.H. Sadhu, C. Mathoniere, Y P. Patil, S.B. Kumar, Polyhedron 122 (2017) 210.
26. Agilent, CrysAlis PRO. Agilent Technologies UK Ltd, Yarnton, England, (2011).
27. G.M. Sheldrick, SAINT, 5.1 ed. Siemens Industrial Automation Inc., Madison, WI, (1995)
28. G.M. Sheldrick. SHELXL-97: Program for Crystal Structure Refinement, University of Gottingen, Gottingen, (1997).
29. L.J. Farrugia, J. Appl. Cryst. 32 (1999) 837.
30. W.J. Geary, Coord. Chem. Rev.7 (1971) 81.
31. J.L. Burmeister, L. Williams, Inorg. Chem. 5 (1966) 1113.
32. A. Turco, C. Pecile, Nature 191 (1961) 66.
33. P.J. Arnold, S.C. Davies, M.C. Durrant, D.V. Griffiths, D.L. Hughes, P.C. Sharpe, Inorg. Chim. Acta 348 (2003) 143.
34. A. Indra, S.M. Mobin, S. Bhaduri, G.K. Lahiri, Inorg. Chim. Acta 374 (2011) 415.
35. K.D. Karlin, B.I. Cohen, J.C. Hayes, A. Farooq, J. Zubieta, Inorg. Chem. 26 (1987)1.
36. K. Nakamoto, Infrared and Raman Spectra of Inorganic and Coordination Compounds, 3rdedn. Wiley Interscience, New York, (1978).
37. U. Mukhopadhayay, I. Bernal, S.S. Massoud, F.A. Moutner, Inorg. Chim. Acta 357 (2004) 3673.
38. M.H. Sadhu, S.B. Kumar, J.K. Saini, S.S. Purani, T.R. Khanna, Inorg. Chim. Acta 466 (2017) 219.
39. A.B.P. Lever, Inorganic Electronic Spectroscopy, Elsevier Publishing

Company (1968).

40. S. Chandra, S. Sharma, Trans. Met. Chem. 27 (2002) 732.
41. B. Chakraborty, T.K. Paine, Inorg. Chim. Acta 378 (2011) 231.
42. J. Matsumoto, T. Suzuki, Y. Kajita, H. Masuda, Dalton Trans. 41 (2012) 4107.
43 M. Kato, H.B. Jonassen, J.C. Fanning, Chem. Rev. 64 (1964) 99.
44. A.W. Addison, T.N. Rao, J.Reedijk, J.V. Rijn, G.C. Verschoor, J. Chem. Soc. Dalton Trans. (1984) 1349.
45. D.-H. Lee, L.Q. Hatcher, M.A. Vance, R. Sarangi, A.E. Milligan, A.A.N. Sarjeant, C.D. Incarvito, A.L. Rheingold, K.O. Hodgson, B. Hedman, E.I. Solomon, K.D. Karlin, Inorg. Chem. 46 (2007) 6056.
46. F. Champloy, N. Benali-Cherif, P. Bruno, I. Blain, M. Pierrot, M. Reglier, Inorg. Chem. 37 (1998) 3910.
47. M. Kodera, T. Kita, I. Miura, N. Nakayama, Y. Kawata, K. Kano, S. Hirota, J. Am. Chem. Soc. 123 (2001) 7715.
48. S. Kim, J.Y. Lee, R.E. Cowley, J.W. Ginsbach, M.A. Siegler, E.I. Solomon, K.D. Karlin, J. Am. Chem. Soc. 137 (2015) 2796.
49. Y. Lee, D.-H. Lee, G.Y. Park, H.R. Lucas, A.A.N. Sarjeant, M.-T. Kieber-Emmons, M.A. Vance, A.E. Milligan, E.I. Solomon, K.D. Karlin, Inorg. Chem. 49 (2010) 8873.
50. S. Kim, J.W. Ginsbach, A.I. Billah, M.A. Siegler, C.D. Moore, E.I. Solomon K.D. Karlin, J. Am. Chem. Soc. 136 (2014) 8063.
51. T.M. Donlevy, L.R. Gahan, Polyhedron 12 (1993) 1593.
52. S.S. Massoud, M. Dubin, A.E. Guilbeau, M. Spell, R. Vicente, P. Wilfling, R.C. Fischer, F.A. Mautner, Polyhedron 78 (2014) 135.
53. A. Solanki, Y. Patil, S.B. Kumar, J. Coord. Chem. 68 (2015) 4017.
54. J. Matsumoto , T. Suzuki , Y. Kajita, H. Masuda, Dalton Trans. 41 (2012) 4107.
55. P. Chaudhuri, R. Wagner, S. Khanra, T. Weyhermuller, Dalton Trans. (2006) 4962.
56. S. Mukherjee, B. Gole, Y. Song, P.S. Mukherjee, Inorg. Chem. 50 (2011) 3621.